Role of Azo Dyes in Reduction of Silver Nanoparticles and their Composite with Reduced Graphene Oxide

Awab Hashmi

Fall-2018-MS Physics

Reg No: 00000278421

A thesis submitted in partial fulfillment of the requirements

for the degree of **Master of Science**

in

Physics

Supervised by: Dr. Faheem Amin

Department of Physics

School of Natural Sciences

National University of Sciences and Technology

H-12, Islamabad, Pakistan

Year 2022

FORM TH-4

National University of Sciences & Technology

MS THESIS WORK

We hereby recommend that the dissertation prepared under our supervision by: Awab Hashmi, Regn No. 00000278421 Titled: Role of Azo Dyes in Reduction of Silver Nanoparticles and their Composite with Reduced Graphene Oxide be Accepted in partial fulfillment of the requirements for the award of **MS** degree.

Examination Committee Members

1. Name: PROF. SYED RIZWAN HUSSAIN Signature: _____

2. Name: DR. FAHAD AZAD Signature: _____

Supervisor's Name DR. FAHEEM AMIN Signature: _____

_____ 18-08-2022
Head of Department Date

COUNTERSINGED

Date: 19.08.2022

_____
Dean/Principal

Dedicated to

My family and friends

Acknowledgements

I would like to express my deepest gratitude to my supervisor Dr. Faheem Amin. I would like to pay regards to my GEC members Professor Syed Rizwan Hussain and Dr. Fahad Azad for their valuable guidance. I am forever grateful to my parents for their support throughout my educational journey. In the, I am very thankful to all my friends and family for their consist encouragements.

Abstract

Metal nanoparticles offer amazing capabilities that have led to the opening of numerous new routes in material science. Metal nanoparticles have the strong chemical activity, high surface-to-volume ratios, optical characteristics, surface plasmon resonance, and adjustable forms as their specialties. Stable AgNPs colloidal particles offer numerous useful uses in the sensors, and the catalytic realm. Creation of stabilized AgNPs is a very demanding work.

This thesis outlines a novel method for synthesizing Ag-rGO: Azo Dye as well as a significant method for preventing particle agglomeration using dyes and GO. Using azo dyes (like Eriochrome Black T, methyl Orange) improves characteristics by acting like a stabilizing agent. After adding GO to the solution, the nucleation processes to capture all free ions, halting the development of the particles, and accumulation of fresh nuclei occurs

The synthesized samples were characterized by various techniques. The formation of silver nanoparticles and reduction of graphene oxide was studied by UV-Visible spectroscopy. At 420 and 260 nm, peaks of silver nanoparticles and rGO were observed respectively. X-Ray Diffraction confirms the FCC structure of Ag and a broad peak of rGO between 10-15^{o}. The SEM images shown the sheets of reduced graphene oxide and stacking of silver nanoparticles over them. EDS suggested the elemental analysis of the composite. Functional groups containing -OH, C = C, C ≡ N and -C-H have been seen via FTIR. The D and G bands in Raman spectroscopy confirmed the presence of reduced graphene oxide with vibrational energy levels.

Further study revealed that Ag-rGO nanocomposite gives a strong degradation efficiency for degrading methylene blue dye. A noticeable growth of the inhibition zone in antibacterial study for both gram-positive (bacillus subtilis) and gram-negative (pseudomonas aeruginosa) strains of bacteria have been observed.

Acronyms

Ag	Silver
NPs	Nanoparticles
rGO	Reduced Graphene Oxide
$AgNO_3$	Silver Nitrate
NaOH	Sodium Hydroxide
XRD	X ray Diffraction
SEM	Scanning Electron Microscope
EDS	Energy dispersive X-ray spectroscopy
FTIR	Fourier transform infrared spectroscopy
EBT	Eriochrome Black T
MO	Methyl Orange
MB	Methylene Blue
UV	Ultraviolet
IR	Infra-Red

Contents

List of Tables

List of Figures

Chapter 01

Introduction

1.1. Nanoscience

The study of superstructures and characteristics of materials on the nanoscale about 1-100nm[1] is called nanoscience When features including size, form, structural, morphological, and surface area of the particle enclosed by the material are scaled down to 10^{-9} of a meters these parameters change the particle's mechanical, kinetics, electronic, optical, photocatalyst, thermal, and magnetic capabilities[2]. The characteristics of nanoscale structures frequently differ from those of macroscale structures. Increased surface area and quantum mechanical phenomena are the driving forces behind this pronounced change in characteristics. [3–5]

1.2. Nanomaterials

The foundation of nanotechnology is nanomaterials[6]. Materials with at least one dimension on the nanoscale scale (100 nm) whether they are crystalline or amorphous, organic, or inorganic display specific features because of the quantum confinement effect. In quantum confinement, electrons are contained within a limited space. Due to their incredibly small size, nanomaterials differ from bulk materials in that they contain discrete (quantized) energy levels as opposed to continuous energy levels. This is because the electronic wave function is limited to the physical dimension of the particle.

Nanomaterials are formed using the following two methods:

1.2.1. Top-down Approach

Using this method, the bulk is successively chopped or sculpted into the appropriate nanostructure. The top-down method has the potential to lead to the improvement of internal

stress, contaminations, and surface flaws[7].

1.2.2. Bottom-up Approach

In this method, the fabrication process entails the construction of material from smaller, inferior units to larger, superior units. This method is used to produce nanomaterials with fewer flaws.[7]

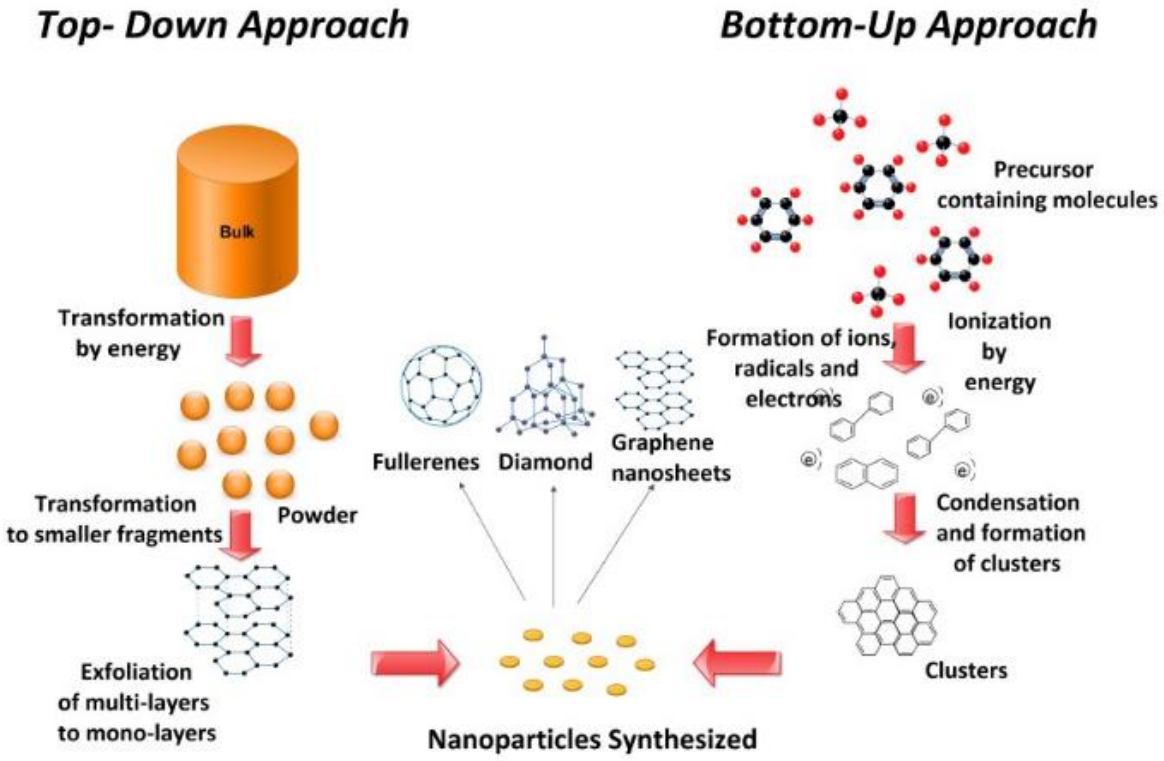

Figure 1.1 Synthesis methods

Nanomaterials are used in a variety of applications because of their remarkable and beneficial electrical, thermal, mechanical, and optical capabilities. As a prospective candidate in applications, nanomaterials are extremely important.[8]

1.3. Nanostructured Material Classification

Gleiter introduced the concept of categorizing nanostructured materials for the first time in 1995[9,10], and Skorokhod expanded on it in 2000[11,12]. The Gleiter and Skorokhod approach, however, was not fully considered because 0-dimensional (0-D) and 1-dimensional (1-D) objects like fullerene, nanotubes, and nanoflowers were not understood[9]. Pokropivny and Skorokhod subsequently reported an improved categorization. which encompasses NSMs in 0D, 1D, 2D, and 3D. Nanoparticles, nanocomposites, and nanofilms are all examples of NSMs. Dimensional analysis is a standard method for categorizing nonmaterial[12]. Nanomaterials are categorized in the following dimensions:

- 0 Dimension (0-D)
- 1 Dimension (1-D)
- 2 Dimension (2-D)
- 3 Dimension (3-D)

1.3.1. Zero Dimension (0D)

The electrons in NSMs are restricted in all three directions as part of a 0-Dimensional system (point-like particles, QDs). As an illustration, consider onions, empty spheres, and nanoclusters, uniform particle arrangements, heterogeneous particle arrays, core-shell quantum dots, nanoparticles etc[13].

1.3.2. One Dimension (1D)

When materials have 2 out of 3 dimensions that are in the nanoscale range (1-100 nm) the electrons in NSMs are constrained in two directions and free to flow in one direction. Examples include nanowires, nanotubes, nanorods, nanofibers, nanobelts, and nanoribbons[14].

1.3.3. Two Dimension (2D)

Two-dimensional systems (quantum wells), in which electrons in NSMs are constrained in one direction but are free to flow in the other two, or nanostructures in which only one of three dimensions is nanoscale is also referred to as two-dimensional nanomaterials. Examples include nanoballs, nanosheets (graphene oxide) nano prisms, nanoplates, nanofilms, and branching structures.[15]

1.3.4. Three Dimension (3D)

There is no confinement of electrons in NSMs, and they are free to travel in all three dimensions in a three-dimensional system (bulk). These materials exhibit more surface area and other superiorities in comparison to bulk materials because of the quantum size effect. These are known as 3D nanomaterials because they often consist of clusters of nanotubes, nanowires, or nanoparticles rather than having any dimensions in the nanoscale. Examples include nanocomposites, nanohybrids, nanometer-sized grains, micro and mesoporous hybrids, nano coils, nanoflowers, nano cones, nanopillars, nanoballs (dendritic structures), etc[16]

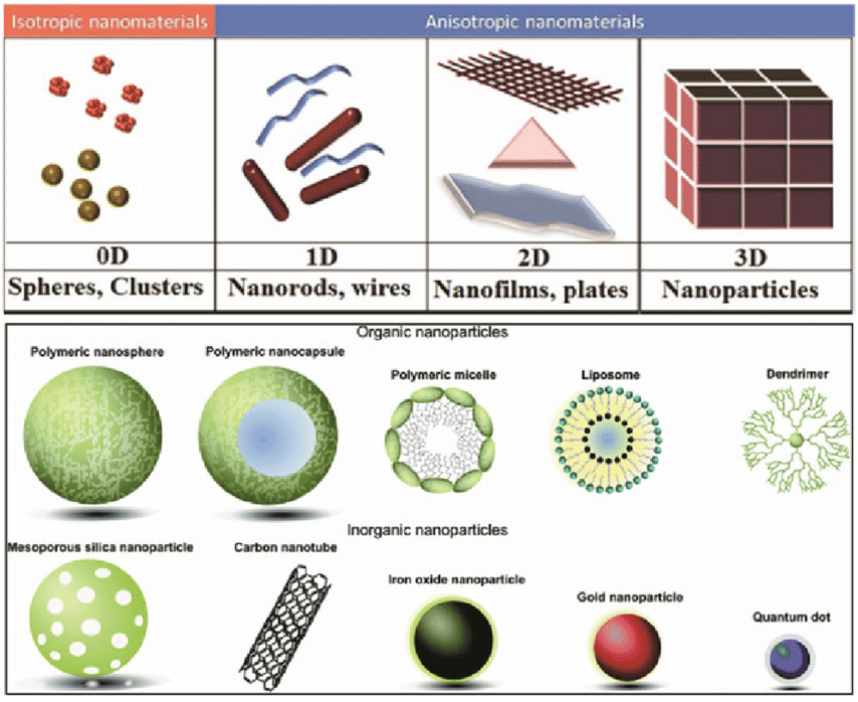

Figure 1.2 Classification of nanomaterials

1.4. Nanomaterials Properties

Due to their exceptional excellence, nanomaterials have sparked a great deal of fascination. The characteristics of nanomaterials differ from those of bulk materials and are strongly influenced by their atomic ratios, shape, and grain size. New quantum effects and a large relative surface area are the two main factors that contribute to the unique features of nanomaterials at scales as small as 10^{-9} of a meter. Electrical, optical, chemical, thermal, mechanical, and magnetic properties will vary depending on how tightly the nanoparticles are contained at the nanoscale.

1.4.1. Electrical and optical properties

Electrical attributes include characteristics like conductance or resistance that rely on the movement of unbound electrons and holes within the atoms. Electronic properties are strongly impacted by the single electron's movement, making it possible to produce single electron devices[17].

When photons are absorbed and reflected separately by particles of varied sizes, they can have distinct hues[18]. For example, bulk-sized gold is yellow, whereas nanosized gold is red in color which is solely due to shift in optical peak absorbance even though same material. As a result, tiny molecules have different optical characteristics than bulk materials. Visible light can be scattered by comparable size ZnO particles, but since nanosized ZnO particles are shorter than the visible light, they are unable to do so. While large ZnO particles were white, nanoscale ZnO particles are clear[19].

1.4.2. Magnetic properties

In comparison to bulk materials, magnetic nanoparticles exhibit a range of unusual magnetic behaviors', primarily because of magnetic or surface connections such as electronic environment, symmetry breakage, magnetic interaction, or charge transport. Even though they are non-magnetic materials like bulk gold, some substances demonstrate magnetic activity at the nanoscale[17].

1.4.3. Chemical properties

The chemical characteristics of nanomaterials can also alter at the nanoscale. Since there are more surface atoms on nanoparticles than on bulk items, their reactivities are higher than those of bulk materials. Nanoparticles contain 50% of their atoms on their surface, hence their electrical characteristics are independent of solid-state bulk phenomena. Atoms in nanomaterials have a higher quantity of energy than atoms in bulk materials because a big fraction of them are found on their surfaces. Because they have a significantly larger surface area than bulk materials, nanomaterial surfaces and interfaces readily capture highly charged species and contaminants, changing their chemical makeup from bulk materials. Composition, molecular weight, structure, vapor pressure, boiling and melting temperatures, water solubility, stability, and reactivity are crucial chemical parameters for defining materials[20].

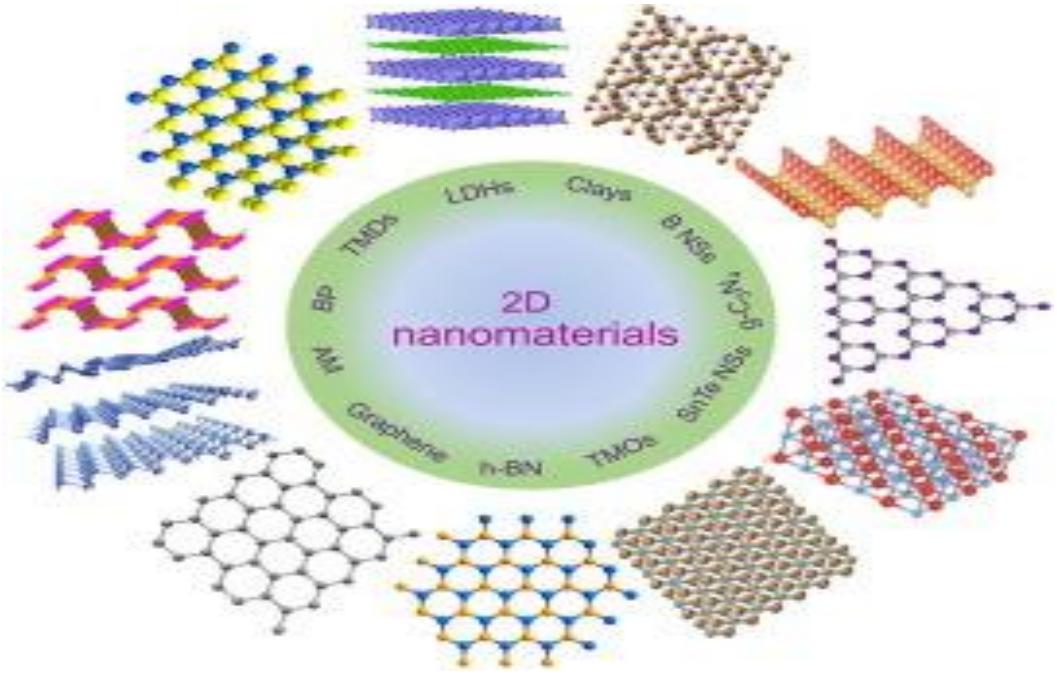

Figure 1.3 Properties of nanomaterials

1.5. Metallic Nanoparticles

Metal nanoparticles have amazing qualities that have opened a lot of new possibilities in the realm of nanotechnology. In addition to having high chemical activity, metal nanoparticles also have enormous surface-to-volume ratios, optical characteristics, SPR (surface plasmon resonance), and adjustable forms that set them apart from bulk k materials[21]. Diffusion occurs more quickly and is achievable in nanoparticles with a greater surface area to volume ratio at lower temperatures. The chemical and physical engagement of nanoparticles with their surroundings, which could be a liquid, solid, or even a polymeric matrix, is improved by high surface area. The optical characteristics of nanoparticles have supported exceptional amounts of interest during the past few decades[22]. Metallic nanoparticles have been employed as ornamental colors since the Roman era. There are numerous examples; the Lycurgus Cup is one of their most significant ones. The cup, which is still on display at the British Museum, has the unique property of changing color depending on the light used to view it. Since the beginning of time, nanomaterials have had a tremendous impact on color. Small nanoparticles were utilized at the time to add color to the church windows. Ruby glass was created using gold and copper nanoparticles, whereas AgNPs turned the glass yellow. He offers an understanding of how metal NPs alter the color of church glass[22] because, before Faraday's explanation, the origin of these colloidal particles was unclear. By lowering the aqueous solution of gold chloride with phosphorus, Faraday was able to demonstrate the creation of a gold colloid. There are also different methods available today for creating noble metal nanoparticles[23].

1.6. Nanoparticles: Uses and Applications

Due to their remarkable characteristics, including their ridiculously small size, huge surface area, and physical, chemical, and mechanical capabilities, nanoparticles have advanced uses in a variety of sectors. The typical ultraviolet sun filter lacks constant stability when in use.

Because they are translucent to visible light in addition to absorbing and reflecting UV light, TiO_2 and ZnO nanoparticles employed as sunscreen offer countless benefits. Because they do have superior UV blocking characteristics than its bulk material, zinc oxide nanoparticles are used in

textiles and sunscreen creams. FeO nanoparticles are employed as a pigment in some cosmetics, demonstrating the importance of nanotechnology in the cosmetics industry[24].

The textile sector has received much interest as one of several other nanoscale materials with the greatest contribution to economic benefit. To increase the flame retardancy, durability, and comfort of textiles, a variety of nanomaterials, such as nanofibers and carbon nanocomposite and nanoparticles TiO_2, Ag, and ZnO, have indeed been altered[25].

Nanoparticles have been demonstrated as a candidate in electrical fabric, military combat apparel, water, and oil repellant, temperature control clothing, composites cloth and substance, and protective clothing due to their low cost of manufacture, antibacterial activity, and UV-blocking capabilities. Because of its effectiveness, nanotechnology has applications in the biomedical field and has drawn the attention of researchers and pharmacists. It is now used in diagnostic instruments, antibacterial agents, analytical tools, and pathogen detection technologies. It is important for organ transplants, genetic manipulation, bio imaging equipment, drug delivery, and bone substitute implants. Additionally, novel nanomaterials have been developed that have the capacity to target malignant cells to operate as an anticancer drug. Nanoparticles also demonstrate how crucial a function they play in tissue reproduction and repair. Gold is used extensively in Ayurveda, Indian healing practice. In some medicinal productions, gold is utilized to improve memory[26].

Electronics like Memory Space, Fiber Glass, Optoelectronic Devices, Screens, Quantum Entanglement[27], and Conductive Coatings are just a few examples of the electrical gadgets that have benefited from the wonders of nanotechnology. Many different electronic gadgets use graphene, semiconductors, and nanocrystals. higher surface-to-volume ratio, better efficiency They are a preferable option for various electronic equipment because of their small size and weight[28].

Large cap and compact batteries were in high demand due to the advancement of laptops, computers, and mobile phones. Nanomaterials, which hold more energy, have a higher energy density, and retain the charge longer than ordinary batteries thanks to their foam-like structure, are employed as separator plates in batteries. Nickel and metal hydride batteries need less recharging and last longer due to the enormous surface area of nanocrystalline materials. Because of their

great electrical conductivity, nanoparticles are utilized for the detection of chemicals like nitrogen oxides and ammonium[29].

Due to their unique chemical and physical properties, nanoparticles are currently the ideal choice to be used in environmental cleanup[30]. Groundwater, air, and toxic soil have all been treated using nano remediation. Redox reactions are the principal purifying method. Industrial effluent nanoparticles are utilized to clean up surface water[31]. Due to their inexpensive cost, smaller amount, stronger responsiveness, increased performance, and thus better performance, nanoparticles have supplanted conventional chemical processes. Nanoparticles are also used to address soil contamination in certain target locations[32].

One-third of the world is covered by land, and approximately two-thirds of it is surrounded by the ocean. One of the most obvious issues people today face around the world is the lack of access to clean water and sanitary facilities. Freshwater reserves are steadily running out, which makes the issue worse. Fundamentally, wastewater is the contamination of water sources like underground water, lakes, rivers, etc. It happens when toxins enter water bodies accidentally or intentionally without receiving the proper treatment to remove the hazardous components. In addition to harming the animals, plants, and other creatures that live in these bodies of water, water pollution also has a negative impact on naturally occurring communities. The value of water is being impacted not only by industrial effluents but also by some natural occurrences like earthquakes, storms, and algae blooms[30–32].

The primary contributors to water contamination are:

- Commercial Discharge
- Excessive Pesticide Use
- Surplus prescription drugs and household sewage
- Organic Substances

A crucial requirement for human health is access to safe, inexpensive water that is devoid of hazardous substances, yet meeting this demand in the twenty-first century is a tremendous issue. Given that no living thing on earth can survive without water, we may understand the significance of drinking water in our life. Most of the water on Earth is marine, and it cannot be treated to make it drinkable. Most of the water on Earth is seawater, that cannot be used for drinking without any

further processing. Fresh water that comes from the earth is really the only water supply. To meet the need for clean water, nanotechnology is playing a critical role. It has made water and sewage treatment more effective, and it also promises to deliver new treatment capabilities that will make it possible to economically use unconventional water sources to increase the quantity of available water. Nano-adsorbents can be used to remove some waste or harmful elements from water. Adsorbents of metal oxides, such as titanium dioxide, iron oxide, and alumina, are effective and priced for removing heavy metals from water[33,34].

1.7. Graphene

Several allotropic types of carbon exist with various physical and chemical characteristics. The crystalline forms of carbon include fullerene (0D), carbon nanotubes (1D), graphene (2D), graphite (3D), and diamond (3D).

A two-dimensional carbon compound called graphene was first described in 2004 by Geim and his colleagues Andre Geim and Kostya Novoselov at Manchester University[35]. In 2010, they received a noble prize for it. Graphene is a unit layer of graphite that is one atom thick. Due to its reduced weight, flexibility, and strength, graphene is becoming increasingly well-known every day. Due to its amazing electrical, thermal, optical, and magnetic capabilities [35], graphene has

taken over the industry in recent years and is now widely recognized as a necessary component of all electronic and optical media.[36]

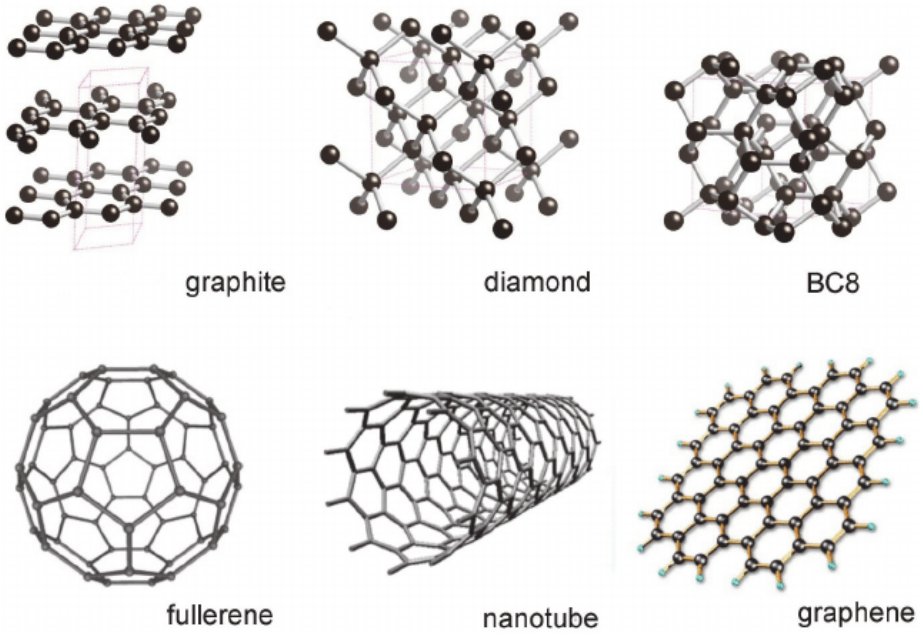

Figure 1.4 Carbon Allotropes

The chemical exfoliation method, which uses graphite as the starting material, is the most straightforward and affordable approach to making graphene[37]. Graphite is turned into multilayer

graphene known as CCG (chemically converted graphene) or rGO using oxidizing and reducing chemicals (reduced graphene oxide)[38].

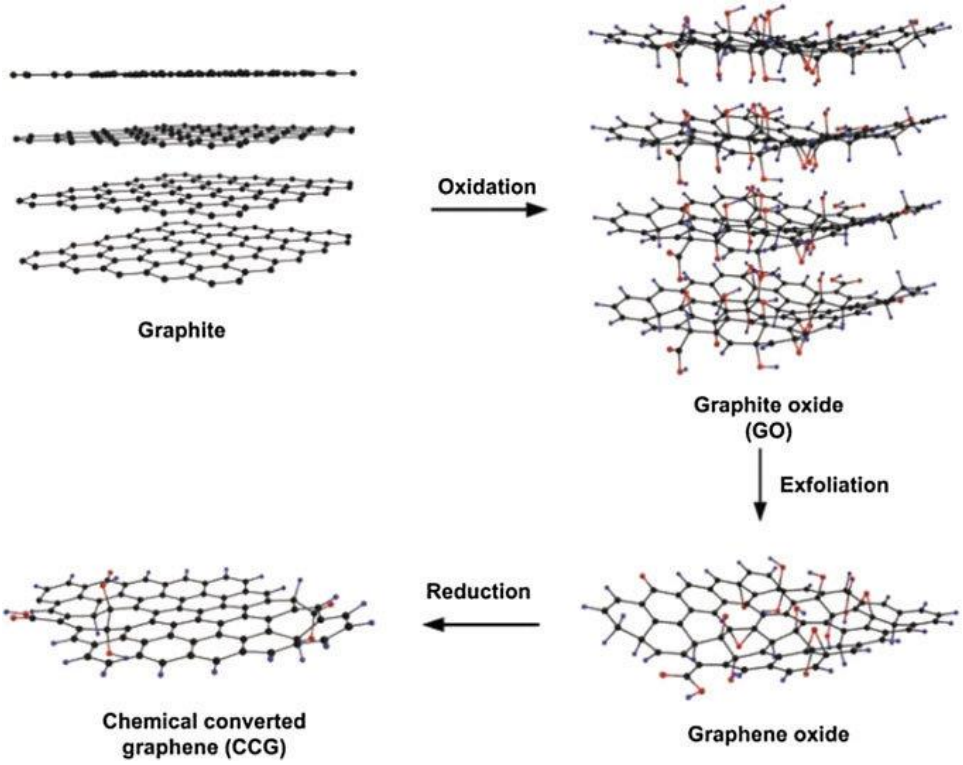

Figure 1.5 Chemical exfoliation of graphene

1.8. GO (Graphene oxide)

Graphene oxide is referred to as GO. Graphite is chemically oxidized to form GO, which is subsequently exfoliated in the proper solvent to make single- or multi-layer GO[39]. Different functional groups, including epoxy, hydroxyl, and carbonyl, are linked to the surface and edges of the graphitic layers because of oxidation. The van der Waals forces among the graphene planes weakened because of these functional groups[40].

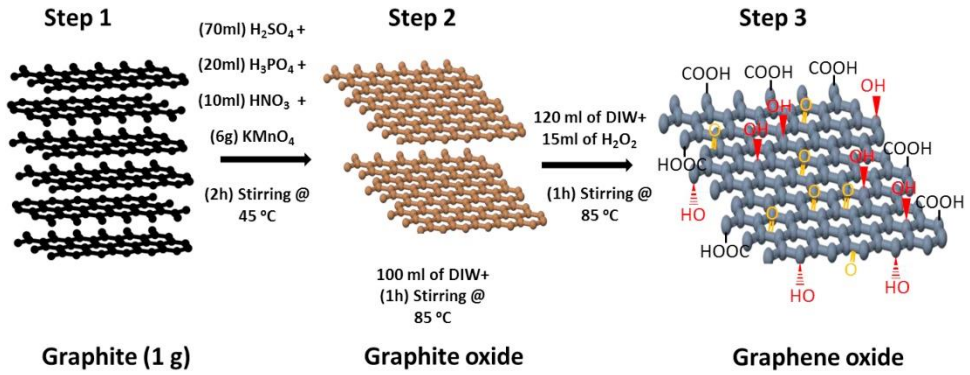

Figure 1.6 Structure of graphene and graphene oxide

Schafhacutle was the first to describe the intercalation of graphite sheets to produce graphite oxide in 1840. There are two diverse kinds of carbon atoms in GO: those that form bonds with various functional groups and those that participate in the production of aromatic rings[41].

The amounts of two sorts of carbon atoms or regions show how much oxidation is done. Both sides of the plane have these functional groupings. These functional groups provide graphene oxide with its hydrophilic character, which allows stable aqueous solutions to develop[42].

The following four procedures are utilized to create graphene oxide:

1. Staudenmaier
2. Hofmann
3. Brodie
4. The Hummers method and its altered versions.

The types of acids and oxidizing agents utilized in these processes to produce graphene differ from one another. Potassium per chlorate, fuming nitric acid, sodium nitrate, and potassium per manganate are used in the Staudenmaier method, while concentrated nitric acid and potassium per chlorate are used in the Hofmann method. The Hummer's method and its modified variations are the widely used procedure for the chemical production of GO. The modified Hummer's method

has numerous advantages over other approaches; it increased graphene oxide yield and graphite oxidation efficiency, and it does not employ $NaNO_3$, preventing the release of harmful gases.

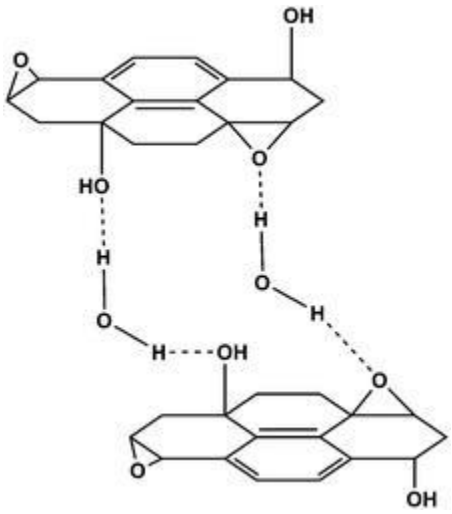

Figure 1.7 Hydrogen bonding in graphene oxide layers

1.8.1. Applications of Graphene Oxide

Due to its remarkable physical, biochemical, electrochemical, and optical capabilities, graphene has aided study and industry. Because it has numerous simultaneous qualities that other materials do not, graphene is valued highly. The excellent conductivity and transparency of graphene make it desirable for usage in a variety of applications. Crystal is transparent but not conductive, while copper is both flexible and conductive. To obtain more than one property, more than one material is employed to create a hybrid structure. These hybrid structures have qualities of both materials to some extent but are difficult or expensive to synthesis. Graphene has an incredibly special electrical structure and set of characteristics. Given that graphene has a zero-band gap, The charge mobility is quite good because to the 0-band gap even at ambient temperature. ITO-structures are a type of hybrid structure. Because they combine two desirable qualities—good electrical conductivity and transparency—metal composites are frequently employed as transparent electrodes in solar cells. They can function as electrodes in solar cells thanks to this characteristic. Due to its dual qualities of transparency and conductivity, graphene can be employed as a transparent electrode without the need for hybridization.

History is full of instances of graphene-based devices. When patterned on the surface of a graphene sheet, nanomaterials with good chemical and thermal stability and a wide surface area have significant qualities that can be used as a gas sensor. Because of its astounding electronic structure, greater surface area, and potential use in the creation of next-generation sensors, graphene is an effective gas absorber. Graphene and GO also exhibit novel mechanical, optical, catalytic, and electronic properties that can be applied to biosensor materials.

For sensor applications as imprinting surface increased Raman spectroscopy (SERS) substrate for 12 molecule detection, pH sensing, humidity sensing, as well as gas sensing, graphene in its various forms, notably GO-based material, have been reported[49,50]. Due to their high energy density, supercapacitors vary from regular capacitors. Supercapacitors were initially made available to the public in 1957. Supercapacitors are used instead of simple capacitors in applications requiring rapid cycle life as they are primarily designed for battery storage. Due to the addition of functional groups containing oxygen in the Go basal plane, GO is not a conductor in nature. 1012 ohm per square is the value of GO's sheet resistance. Because of sp3 flaws that have been inserted into the structure, graphene has an insulating quality. These flaws render GO non-conductive by interfering with carrier transport between sp2 hybridized carbon clusters. However, by reinstating the sp2 coupled network of graphene, GO can be converted into a semiconductor. This reduction process uses a variety of technologies, including chemical, thermal, electrochemical, etc. The element of the removal process plays a vital part in evaluating the efficacy of the removal process. By breaking down the oxygen functions and restoring the sp2 hybridization of carbon clusters, thermal treatment also improves electrical conductivity[51,52]. In a study, it was discovered that the concentration of sp2 and the amount of oxygen in a totally reduced GO were 80 and 8 percent, respectively. Charge carriers cannot be transported because of the leftover oxygen[52,53].

The internal strength of graphene was measured using nanoindentation in AFM and was determined to be 1.0 TPa and 130 GPa, respectively [53]. AFM was used to assess the mechanical qualities of sheets made of GO. When graphene oxide's monolayer was 0.7 nm thick, Young's modulus was discovered to be 207–23.4 GPa. The addition of functional groups containing oxygen causes the 2D structure of graphene to change, which lowers the strength of graphene oxide relative to graphene. The addition of functional groups alters the binding energy and molecular structure

of graphene, causing the sheets to become unstable [52],in consequences GO's elastic characteristics reduced. The heat transfer of GO is similarly decreased by the insertion of sp3 defects. Graphene's special qualities make it possible to create low molecular polymeric materials with high strength for usage in a variety of industries, including aerospace, automotive, food packaging, and electronics.

1.9. Nanocomposites

A nanocomposite is a fusion of two materials created in a way that allows us to access their superior capabilities. When it comes to nanocomposites, one of the phases should be in the nanoscale [42,43]. Composites typically contain two phases: the matrix phase and the reinforcing phase. In nanocomposites, various nanometer-scale building blocks are employed to produce novel materials with superior electrical, physical, optical, and catalytic capabilities. When it comes to graphene-based nanocomposites, the product contains multiple phases, one of which is a matrix and the other of which is a discontinuous phase (often arranged in the form of sheets, particles, or fibers)[44]. Materials for nanocomposites are increasingly being considered an appropriate option for overcoming all the restrictions that micro composites encounter in various applications. Due to its hydrophobic nature and higher surface energy, graphene cannot be consistently disseminated and is frequently inappropriate for use with all available organic polymers. Therefore, evenly distributing the graphene sheets throughout the polymer matrix presented a significant problem for the researchers. Functionalization or chemical alteration are employed to create stable graphene suspensions or homogenous graphene distribution. Materials based on graphene's, such as GO and rGO, are the clear other choices in this environment.

The simplest structures are made by combining lesser amounts of graphene with metals, polymers, or ceramics to create nanocomposites. The two-dimensional graphene oxide system contains two distinct areas, according to the Lerf-Klinowski model[44,45]. The second region is made up of oxygen-containing functionalities, comprising hydroxyl and epoxide groups at the basal plane and carboxyl and carbonyl groups on the margins. The first section is made up of sp-2 hybridization carbon domains.

Due to the ease with which GO sheets can be dispersed in polar solvents, these functional groups enable the formation of stable dispersions. These nanomaterials will be significantly stronger,

more heat resistant, and more conducive thanks to the incorporation of graphene. GO can function as an ion-exchange resin by exchanging ions with metal cations due to the presence of ionizable carboxyl groups[46]. These characteristics allow metal or metal oxide NPs to be anchored on the edges and surface of GO, acting as a support for the 2-D structures of GO [47]. There is a significant band gap between both the sigma-states of the sp3 domains that are related to functional groups that contain oxygen and the conducting pi-states that result from the presence of sp2 domains. The electrical structure of GO is diverse because of these two elements. Therefore, the electrical characteristics of GO can be changed from insulating to semiconducting by altering the carbon to oxygen ratio[48].

1.10. Objective and Structure of this Work

This thesis explains the synthesis of Ag-rGO composite using top-down approach. Azo dyes (Eriochrome Black T and Methyl Orange) have been used as reducing and stabilizing agents for the preparation of composite. Steps of synthesis involves stirring and sonication of silver nitrate, graphene oxide and azo dyes. After sonication, obtained solutions were washed by centrifugation. All the experimentation has been performed at pH 9.

1. Synthesis of Eriochrome Black T capped Silver Nanoparticles and its composite with reduced graphene oxide.
2. Synthesis of Methyl Orange capped silver nanoparticles and its composite with reduced graphene oxide.
3. Characterization of synthesized composites (UV-Visible, XRD, SEM, EDS, Raman, FTIR).
4. Applications of Ag-rGO composite (Photocatalytic dye degradation using Methylene blue as a dye and Antibacterial activity for gram-negative and gram-positive strains of bacteria).

Chapter 02

Literature Review

2.1. Graphene History

Graphene has a long history; it first came to public attention in the nineteenth century. The first person to discuss graphene was Canadian physicist Philip Russell Wallace in 1946[54].Wallace was interested in studying graphite, the substance used in lead pencils, and had no idea that it was possible to create graphene. Graphite, a material composed of carbon atoms and resembling a 3-D honeycomb. C atoms are arranged in hexagons on a two-dimensional grid in graphene. Wallace demonstrated how graphite can be produced by stacking graphene sheets.[55,56]

Wallace used his graphene calculator to generalize knowledge of graphite. Wallace is only vaguely aware that his hypothetical content could be produced in the real world. He extrapolated data about graphite using his estimations for graphene. Wallace is only vaguely aware that his hypothetical content could be produced in the physical world[57].

Wallace's Graphene was created in 2004 by physicists Andre Geim and Konstantin Novoselov using the scotch tape method. The first layer of carbon atoms was identified and separated by researchers Andre Geim and Kostya Novoselov from the University of Manchester. They received the 2010 Physics Nobel Prize in recognition of their accomplishment. They created Wallace's theoretical material in the real world. Following that, both the scientific and financial communities were affected by the discovery of graphene.

The most straightforward and affordable method of producing graphene is through chemical exfoliation, which involves oxidizing graphite. The Brodie, Staudenmaier, Hofmann, Hummer's method, and modified variations of the Hummers method are some crucial techniques utilized for GO synthesis. In these processes, graphite powder combines with acids (such as hydrochloric, sulfuric, and nitric acids) as well as some alkali metals (such as $KClO_3$, $KMnO_4$, $NaNO_3$, etc.). As a result of this reaction, the graphite powder transforms into graphitic layers. After oxidation, it

can be reduced by reducing chemicals; therefore, in this process, graphite can be transformed into multilayer graphene, also known as chemically transformed graphene and rGO.

Graphene is currently getting a lot of interest from researchers in the hope of finding a practical application. There is no surprise that many scientists are eager to make the significant discovery that could be recognized for its contributions to science because almost a decade of investigation on graphene has secured significant potential to superb electronic characteristics, exhibit strong photo catalytic activity and larger surface area in application domains such as circuitry, rust protection quite effective solar cells , longer-lasting battery packs, medicinal technologies such as pointers of diseases, and screens[58].

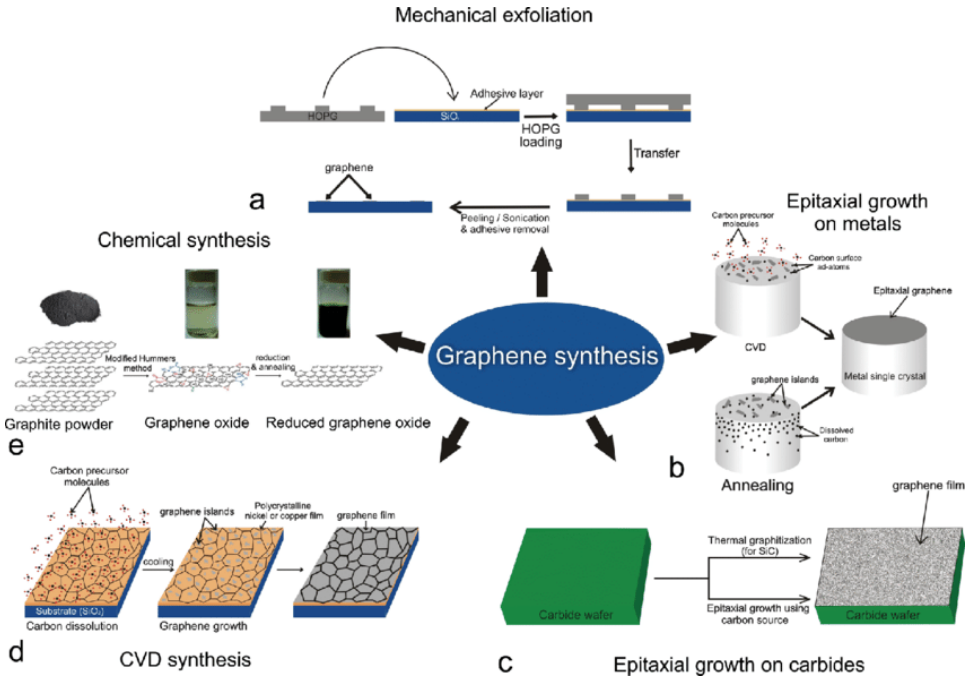

Figure 2.1 Synthesis of graphene

2.1.1. Structure of Graphene

Carbon nanotubes, diamond, graphite, and fullerene are allotropes of carbon that also include graphene. Graphene is the first completely crystalline 2-D material to be created, and it serves as a model for the subsequent generation of 2-D materials like different layers of BN and MoS_2. The electrical structure of well-known 3-D materials differs from that of graphene. Graphene is made up of carbon atoms with a hexagonal configuration. The C atom has four electrons in its

outer shell, each of which has three electrons and forms a chemical bond with its nearest neighbor's electrons. The 4th electron is displaced for every atom throughout the whole graphene layer, allowing for the conduction of the electric charge. Each carbon forms a sp-2 hybridized sigma bond and one pi bond.

Electrons in insulators and metals have various energy levels. Insulators are referred to be non-conducting materials because of the energy gaps that spread their entirely full or empty energy levels. Metals with one band that is only partially filled. The bands resemble parabolas if the function of momentum is employed to describe the energy of e. The energy zones that design two circular cones side by side at their ends behave unusually in graphene. Graphene's Fermi region, seen in Figure above, has six double cones. The Fermi level of a fundamental graphene is located at the intersection of these cones. They are referred to as "Dirac cones." For positive charge carriers and negative charge carriers close to the Fermi level, the frequency dependence is linear. Energy bands do not have gaps like insulators do, nor do they have partially full bands like metals do. Due to the obvious cones, the graphene electrons behave in a very odd way. All the electrons have the same velocity and completely lack inertia. Electrons have little mass. Since effective masses are determined by the curves of the energy levels, graphene electrons have no effective mass. The equation that describes the excitation in graphene is the same as the Dirac equation for fermions, which has no mass and moves at an unchanging speed. Because of this, these cones' link points are also referred to as Dirac points. This allows us to draw some fascinating comparisons between graphene and particle physics. Which are acceptable up to 1 eV, as it proceeds to be nonlinear.

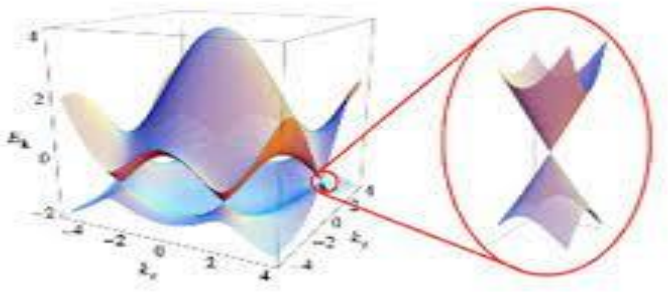

Figure 2.2 Graphene energy-dispersion relation

2.1.2. Graphene characteristics

The continuously expanding body of scientific literature provides extremely strong validation for the amazing graphene characteristics. Here, some of its intriguing characteristics and potential scientific applications are explored. The Graphene layer is impermeable to every molecule, including tiny ones like helium molecules. The formula yields the conductance of a layer for 2-D materials, $\sigma = enu$. At a carrier concentration of $n = 10^{12}$ cm^{-2} graphene indicated a strong movement of charge-carrier in the region of 2000–5000 cm^2 /V s [59]. This is the suspended graphene layer's charge transport, which in an ideal environment would be greater than 200 000 cm2/Vs[60] . Uses like FETs, which then in 2010 could operate at frequency range as high as 100 GHz, and many more recently, graphene field-effect circuitry, which can operate at thz frequencies, show the potential impact of an amazingly permissive charge transfer material.

The heat transfer of graphene is dominated by carriers of heat , and it is estimated to be around 5000 Wm -1 K -1, for Cu it is roughly 401 Wm -1 K -1 at standard room temp. Due to its enormous unique surface size of 2630 m2 g-1 and greater Young's modulus of 1 TPa ,graphene's heat transfer is 10 times better than that of copper.

Graphene can absorb 2.3 percent of the light intensity or, in the opposite case, offers an extraordinarily high optical clarity of up to 97.7 percent; it is practically clear in the optical domain and is wavelength agnostic. This value is provided by $\pi\ \alpha$ (where α is the fine structure constant). Graphene in suspension is hence colorless. These qualities could be advantageous in solar cells as electrode materials[61].

2.2. Metal Nanoparticles

Metallic nanomaterials are less than micrometer sized objects formed of metallic materials (such as iron, calcium, zinc etc.) or their compounds like sulfides. For use in environmental, medical, catalytic, antibacterial, photographic, biosensor, electrical, and optical applications, metallic nanoparticles are very appealing. Because of their structural continuity across molecules and in bulk, nanoparticles bridge the gap between surface-related science and molecular science. It was shown in the previous section that materials exhibit unique physicochemical properties at the nanometer size compared to bulk. These characteristics are very positive for a wide range of

technical applications. The most fascinating and advantageous aspect of nanomaterials is their optical characteristics. These particles' optical characteristics are quite interesting, and they rely heavily on a strong visible absorption band known as the SPR plasmonic band, which is a characteristic of the dispersing of Au, Ag, or Cu. Lasers, biosensor, visual sensors, imaging, photovoltaic cells, screen, photo catalyst, and healthcare are a few applications based on the optical characteristics of metallic nanoparticles.[62–64]

Colloidal nanomaterials with diameters in the nanoscale to micrometer region were created recently via solution techniques. The shape and geometrical makeup of the nanomaterials was examined using microscopic methods. The properties of metal nanoparticles (NPs) differ from those of bulk materials made of the same atoms. With the reduction in NP thickness and an increased proportion of surfaces of different atoms, the ratio of surface to inner atoms rises[65–68].

2.2.1. Optical Properties of Metal Nanoparticles

As the material's size decreases, its optical characteristics alter significantly. Each metal reveals its distinctive color. Gold microspheres appear violet or red in the nanometer level in fluid solutions, as opposed to the bulk metal. Palladium and platinum nanocrystals are dark in color. Silver nanocrystals have a yellow color in liquid[69]. The vivid colors that noble metals own NPs are in a higher energy level because photons with the appropriate frequency, which is caused by the combined vibrations of the conduction level electrons. The shape, chemistry make-up, and surrounding dielectric atmosphere all have a significant impact on the optical characteristics of NPs. These qualities can be deliberately modified to fit a particular application. Surface plasmon resonance is among the causes of their special characteristics. The optical qualities can be significantly employed for enhancement purposes, including in biomaterials, materials for higher potency collecting optical disks, optoelectronic gadgets, and biochemical sensors[70].

2.2.2. Surface Plasmons

The positively charged particles present in metals are surrounded by lots of electrons. The free negative charge carriers appear like a fluid and flow because of the application of an electric field. The negative charge carriers would vibrate in the fluctuating field. An EM radiation has quite a

specific penetration depth on a metal surface known as the skin depths. Au and Ag, it is 50 nm, hence only the metal surface negative charge carriers are significant for their combined vibrations known as surface plasmons. Electron vibrations are quantized and resonant at a specific frequency. Plasmons are the name for such fluctuations. Plasmons are free negative charge carriers from coherence excitations in a metal. The kind and form of the particle material all affect the plasmonic frequency. It is connected to E=hf. The interplay of plasmon with incoming particles of light dominates the optical characteristics of metal NPs. Silver and other nanostructured materials have plasmon frequency that are visible. White light with a range that matches the plasmon resonance absorbs when it strikes metallic nanoparticles. For a specific particle, its size and shape determine the intensities, spectrum positions, and the quantity of plasmon resonant frequencies[1971].

Interactivity of photons and electrons of NPs of metal. Above given figure shows how metallic nanoparticles' photons and negative charge particles interplay. SPR occurs unless a nanoparticle's dimension is substantially smaller than the incident light's wavelengths. The EF is caused by the incoming light to push the negative charged particles in one direction out from the other particles and generate an electric dipole. As a result, there is a net negative charge with one end and a positive charge on another.

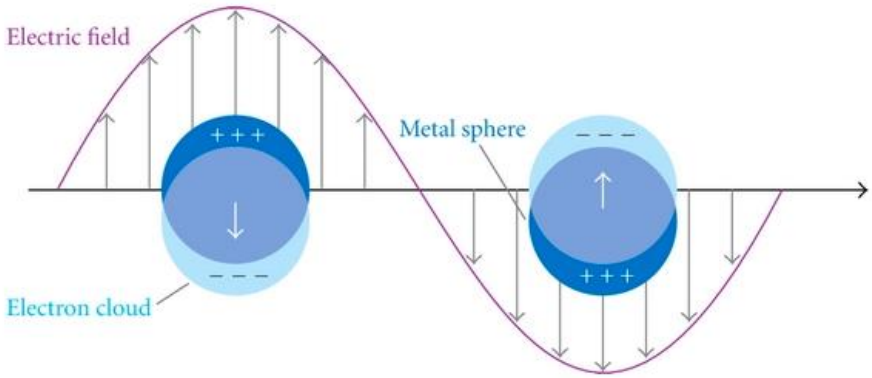

Figure 2.3 Metal particle electrons interaction with light.

The intensity, location, and form of SPR are strongly influenced by the mono dispersity, shape, and size of NPs. Additionally, the makeup of the environment, the basic interplay among

nanomaterials and stabilizing ligands, and the features of SPR can all have an impact. Due to a reduction in the length of the metallic NPs or a rise in temperature, red changes appear in the SPs levels. The charge carriers enhance the scattering rate as a consequences of a nanoparticle's size change, which ultimately causes the stochastic red shifting of the SPR. The below given figure displays the findings of the studies with colloid Au of the SPs levels with different sizes. According to the graph, we could see that the frequencies of its level drops as particle size increases[72].

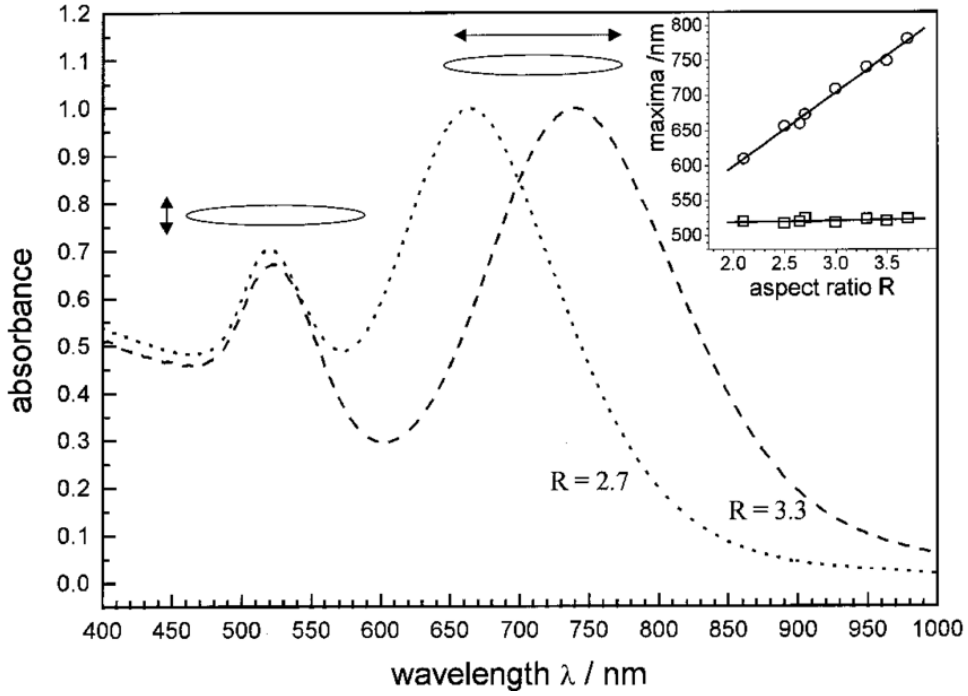

Figure 2.4 Au particles plasmon band

2.2.3. Particle Shape

The aggregates of colloid metallic NPs are incredibly pompous in terms of plasmonic absorption and frequency. The plasmon level moves to a longer wavelength and the plasmon frequency decreases because of the accumulation of such metallic NPs [73]. AgNPs in the range of 10 to 20 nm exhibit their typical 400 nm absorption. AgNP aggregates increase the absorption maxima near 520 nm, which causes the strength of plasmon absorption to drop.

The plasmon absorption moves to higher wavelength and the plasmon frequency drops as a result of the aggregates of colloid metallic nanoparticles. For instance, in water, AgNPs of size (10–20

nm) exhibit plasmon absorbance at about 400 nm. AgNPs group together, causing a drop in plasmon absorption values and the appearance of a wide maxima at 525 nm.[74,75]

2.3. Preparation of Noble Metal Nanoparticles

Metal nanoparticles' optoelectronic characteristics have a clear relationship with their scale, exterior chemical, form, aggregation activity, and surroundings. Due to their remarkable electrical, thermal, and refractive indices, these nanoparticles have garnered a great deal of scientific and engineering attention[76].

Numerous biological, chemical, and physical processes can be used to create noble metallic nanoparticles. The extraordinary qualities of these metallic nanoparticles include their protection against rust, oxidation, non-reactivity, great potency for reducing, and higher melting points.

Metallic nanoparticles are prepared using a variety of techniques, including photochemistry reducing, heat evaporating, chemical reduction methods involving reducing agents, and electrochemical treatment. A highly energetic laser is used to physically evaporate atoms from the metal surface, and then these atoms are cooled to form nanoparticles (NPs). Compared to chemical methods, physical methods for the synthesis of metal nanoparticles are more challenging since they call for high temperatures, vacuum, and expensive equipment. While using inexpensive equipment and diluted standard solutions, methods usually are simple to implement[76,77].

2.3.1. Reducing Agent

Adjusting the reductant, the dispersion agent, it takes for the reaction to occur, and the temperature, it is possible to precisely control the arrangements and form of the NPs after implementing the chemical reduction process. The process of chemically reducing metal ions to their zero oxidation states (i.e., Mn^{+} to M_o) is carried out by the chemically reducing method. It requires simple equipment and may quickly and affordably create higher quantities of NPs[78,79].

Typically, salts of metals and reductants interact to form metal NPs. Chemically reducing activity happens whenever they interact with metal salts. according to equation

$$mMe\ n+ + nRedu \rightarrow mMe\ o + nOxid$$

The table below lists the most often employed reducing agent under suitable conditions for such salts of gold, silver, and copper.

Table 1 Reaction conditions for reduction processes.

Metal Species	E^o/V	Reducing Agent	Conditions	Rate
Au^{3+}	$\geq +0.7$	Alchohol, Polyols	$\geq 70^oC$	Slow
Ag^+		Aldehydes, Sugar	$< 50^oC$	Moderate
		Hydrazine, H_3PO_2	Ambient	Fast
		$NaBH_4$, Boranes	Ambient	Very Fast
		Citrate	$> 70^oC$	Moderate
Cu^{2+}	< 0.7 and ≥ 0	Polyols	$> 120^oC$	Slow
		Aldehydes, Sugar	$70 - 100^oC$	Slow
		Hydrazine, Hydrogen	$< 70^oC$	Moderate
		$AnBH_4$	Ambient	Fast

2.3.2. Ag Nanoparticles Synthesis

Degradation efficiency of metallic ions would be used to create metal nanoparticles in liquid. Ag salts are reduced to form AgNPs. Silver nitrate is primarily utilized as a precursor material. AgNPs can be produced via reduction techniques, and the choice of reductants, swirling rate, temperature, and reactivity duration can all change. The circumstances of the chemical process determine the color and size of the silver nanoparticles. By reducing $NaNO_3$ with $Na_3C_6H_5O_7$, AgNPs in the 40–60 nm size category is produced at boiling temperatures.[78,80]

Through reducing $AgNO_3$ with ice-cold $NaBH_4$, Ag nanoparticles of 10 nm size are created at required temperature for one hour. The highest amount of absorbance was at a wavelength of 400 nm, and the silver nanoparticles were brown or yellow green in color. Green color NPs with sizes between 65 and 85 nm and maximum absorbance at 438 nm are produced when AgNPs are

generated at boiling temperatures with $Na_3C_6H_5O_7$ and $NaBH_4$. Depending on how long the reaction takes, yellow Ag nanoparticles can be produced using ice-cold $NaBH_4$[81–85].

Chapter 03

Characterization Techniques

After the synthesis process, next step is to analyse the different properties of the material including its structure, morphology, and its electrical properties. So different characterization techniques are used to investigate the different properties of the materials. Moreover, the working principle of different characterization techniques are also discussed.

Figure 3.1 Characterization techniques.

3.1. X-Ray Diffraction (XRD)

X-rays are the electromagnetic radiations and provide critical information about the material research. X-rays have shorter wavelength than that of the visible light. It is an analytical technique used for the study of the present phase and crystal structure of a material and it a non-destructive tool. It is also used to investigate lattice constants, translation symmetry, crystal defects, shape, microstructure analysis of polycrystalline specimen, interplanar distance and crystallite size using Scherrer formula ranging from fluids to powder and crystal[86].

3.1.1. Working Principle of XRD

When monochromatic X-ray incident on a material constructive interference produces. X-ray diffraction is based on this constructive interference which produces a diffraction pattern. The conditions in which constructive interference occurs can be provide by the Braggs law, which is the basis of XRD[87,88].

$$n\lambda = 2d\ \sin\theta$$

Where n is the integer corresponding to the order of reflection, λ is the wavelength of the radiation used, d is the interplanar spacing and θ is the scattering angle. The detector is placed at an angle 2θ to the incident X-ray. The results are usually presented as the intensity vs. 2θ. From the position of intensity peak it is possible to calculate d_{hkl} according to the Bragg's Law. In the specific case of MXene the (002) plane, corresponding to h=0 k=0 and l=2, diffracts and is one of the most intense peaks observed. The 2θ position of this peak is therefore used to determine the c-lattice parameter.

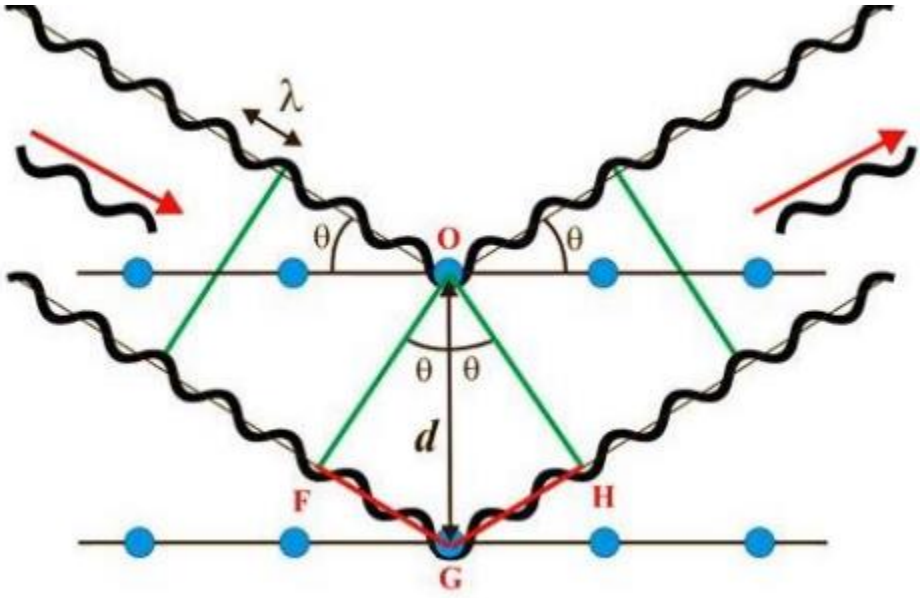

Figure 3.2 Working principle of XRD

So, when the sample is placed on the specimen and detector at angle of 2θ, the diffraction beams that are scattered at all sides are recorded, peaks appeared only when the Bragg's condition is

fulfilled, and these peaks determined the crystalline or amorphous nature of the material. Moreover, the particle size can also be calculated by using Scherrer formula.

$$t = \frac{K\lambda}{A\,Cos\theta}$$

where t is the mean size of the particle, K is the dimensional Scherrer constant, λ is the wavelength of the incident ray, A is the line broadening at full width at half maximum.

3.2. Raman Spectroscopy

Raman spectroscopy is based on an effect known as Raman scattering presented by C.V Raman and K.S. Krishnan in 1982. This spectroscopy is based upon inelastic scattering of incident monochromatic light from the sample. In this spectroscopy, the sample is irradiated by strong laser source in UV-visible region and scattered light is observed at perpendicular direction to the incident beam.

Main parts of the Raman spectroscopy are laser excitation source, excitation delivery optics, collection optics, wavelength separation apparatus, detector , recording device and sample material.[89,90]

3.2.1. Scattering Mechanism

When monochromatic light falls on the sample material with frequency ν_i, some of the light absorbed and remaining part of the light transmitted. When light is in the direction perpendicular to the sample material some of the light is scattered with frequency ν_f. There are two cases, first case is known as Rayleigh scattering that occurs when $\nu_i = \nu_f$ and excited electron returns to its initial state. Second case is Raman scattering that occurs when $\nu i \neq \nu_f$ and scattering can be thought of two wave phenomena. As electron resides at different vibrational levels, if an electron excited to certain level after absorbing the incident light, it will be de-excited. So, if electron falls back to its different levels, it emits a photon of different energy. This gives rise to Raman Stokes and anti-stokes shift[91–93].

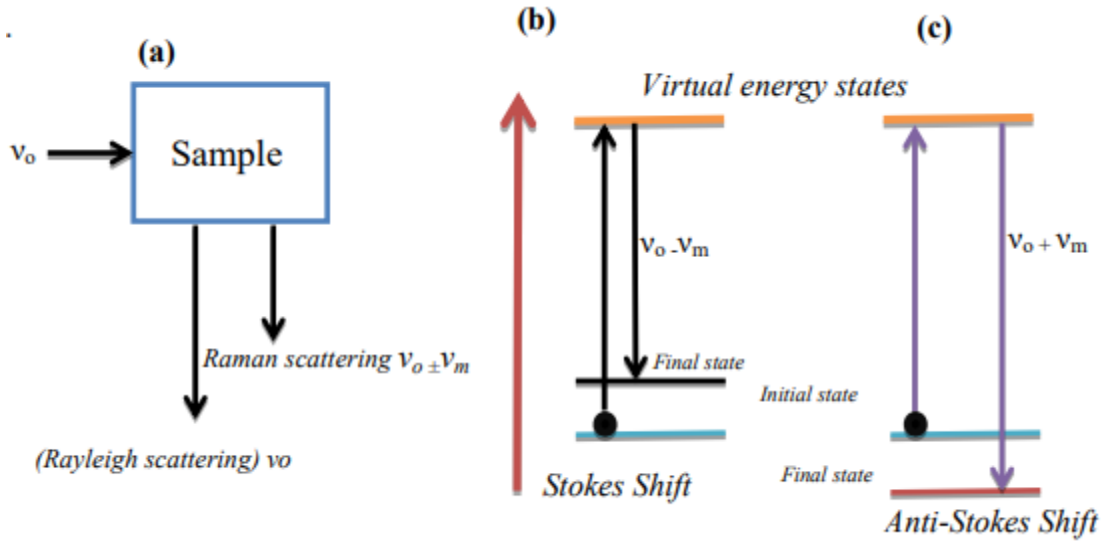

Figure 3.2 Raman scattering energy level diagram (a) Mechanism in Raman Spectroscopy (b) Stokes shift (c) anti stokes shift.

Scattering provides data that is converted into wavenumber and wave number difference is obtained with the incident light. This difference is given on x-axis while Raman intensity is given on y-axis. In Raman spectrum, peak position indicates the molecular structure, forward/backward shifts in the peaks shows stress in structure, width of the peak show's crystallinity while height of the peak indicates the concentration of substance respectively[90,94].

3.3. Scanning Electron Microscopy (SEM)

Scanning Electron Microscopy is a non-destructive technique used to observe and characterize the external morphology and topographical characteristics of the material on a scale ranging from nanometre (nm) to micrometre (µm) and magnified three-dimensional images of the surface is obtained. High electron beam interacts with the material placed on the specimen and the signals are recorded by the detector which helps us to investigate the morphological analysis of the sample material and the resolution power was estimated to be 1nm[95].

3.3.1. Equipment

Main parts of the SEM apparatus are electron gun, anode, condenser lens, magnetic scanning coils, specimen stage and secondary electron detector.

3.3.2. Working Principle

The electron beam is produced thermionically by the tungsten filament cathode of an electron gun. The interaction between material and the electron beam produces various types of radiation (electrons, X-rays, and fluorescence). Specialized detectors collect the secondary electrons which are low-energy electrons (<50eV) ejected from the k-shell of the atoms at the surface of the material. An image is created by scanning the material surface with the electron beam and recording the number of secondary electrons detected.[95]

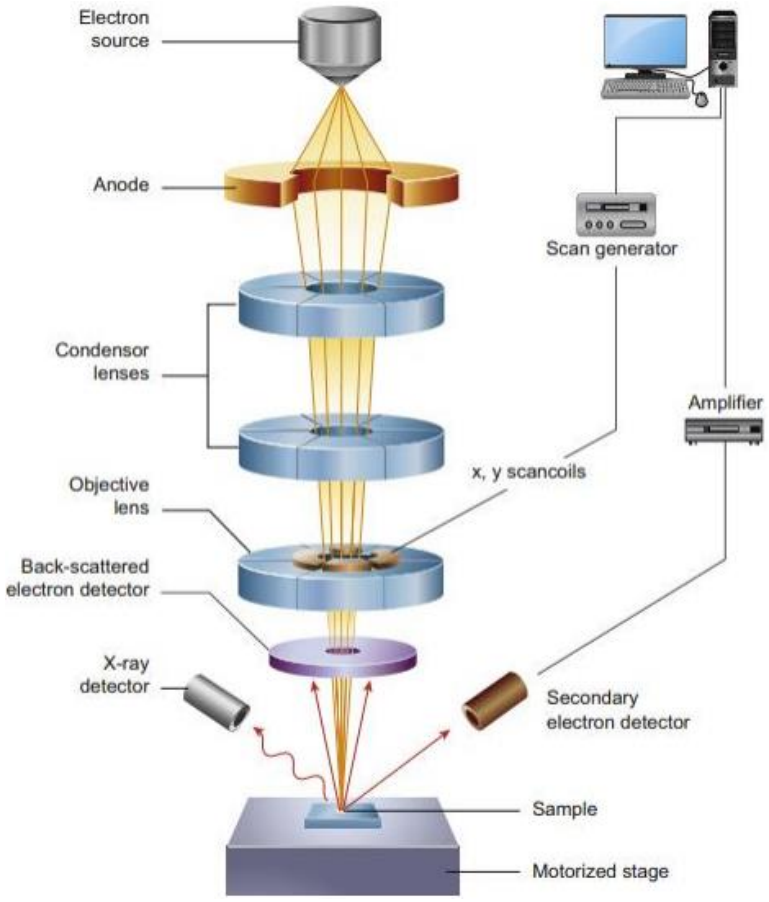

Figure 3.4 Schematic representation of SEM and its working phenomenon

3.4. Energy dispersive X-ray Spectroscopy (EDS)

Energy dispersive X-ray spectroscopy is a technique used for the elemental analysis and in our case, it is presented in SEM for the compositional analysis. X-ray detector is used to record the number and energy of X-rays produced in the sample studied during irradiation by an electron beam. The energies of the X-ray emitted are converted to measure the elemental composition of the sample. The sample in specimen chamber SEM when interacts with a high energy electron beam during EDS Analysis. The electrons which incident from electron column penetrates in the sample and knock out inner shell electrons of the sample, the electrons which are knocked from the internal shell leave a space behind it and this space is then occupied by outer shell electrons. As the electron fills the space from outers shell it gives its energy by emitting the X-rays. The energy which is released depends upon the shell from which electron is out and then relocated. In addition, each element's atom releases X-rays during the transfer process with unique amounts of energy. Now by collecting and measuring the overall energy released by the sample in the form of X-rays, it can identify the atoms. EDS spectrum shows the peaks analogous to the energy levels. Each of the peaks in this spectrum is exclusive for an atom of a single element. The concentration of elements can be known by the length of the peak in the spectrum, higher the peak more weight percent of the elements present in the sample[96–99].

3.5. UV-Visible Spectrometer

This spectrometer is used to measure when light falls on the sample whether it passes or reflected through the sample. The light beam that is used for this technique must be in electromagnetic range in visible and ultraviolet, ranging from 190 nm to 400 nm for visible and 400nm to 800nm for ultraviolet. This spectroscopy is used to measure quantitative measurement. Vacuum condition is necessary to be achieved in this spectrometer for measurement[100,101].

3.5.1. Working Principle

UV-spectrometer follows the Beer-Lambert Law which states that ‘absorbance of the UV-light by the sample is directly proportional to its concentration with its dependence on path length of the cuvette’.[102,103]

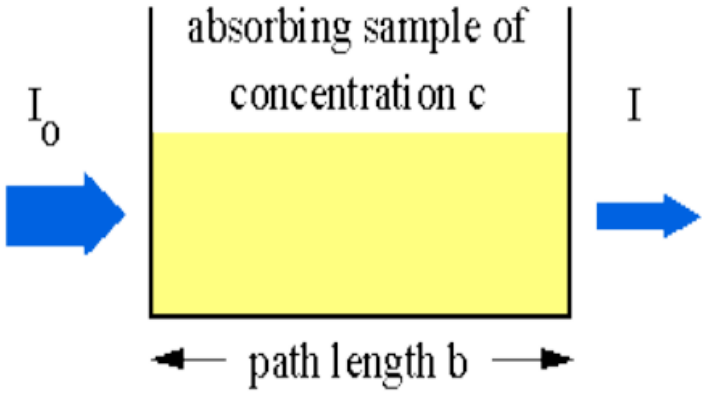

Figure 3.5 Schematic illustration of Beer-Lambert Law

Mathematically, this law is expressed as

$$A = \varepsilon \times c \times l$$

Where

A = Absorbance

Ɛ= Molar extinction coefficient ($dm^3\ mol^{-1}\ cm^{-1}$)

C= Concentration of solution ($mol\ dm^{-3}$)

l= optical path length (cm)

3.5.2. Working of UV-Spectrometer

Mostly two samples are used in this spectroscopy. One sample is a reference sample in which, yet the sample material is not added and other is sample under test both the sample are mostly liquid and are in cuvettes.

First, the reference sample is exposed to ultra-violet and visible light and the amount of the rays adsorbed is noted. Afterwards light is passed from the test sample. Some of the light is reflected and some absorbed. When light is absorbed, the electron jumps to a higher orbit and makes the transition. The detector measures the wavelength[100].

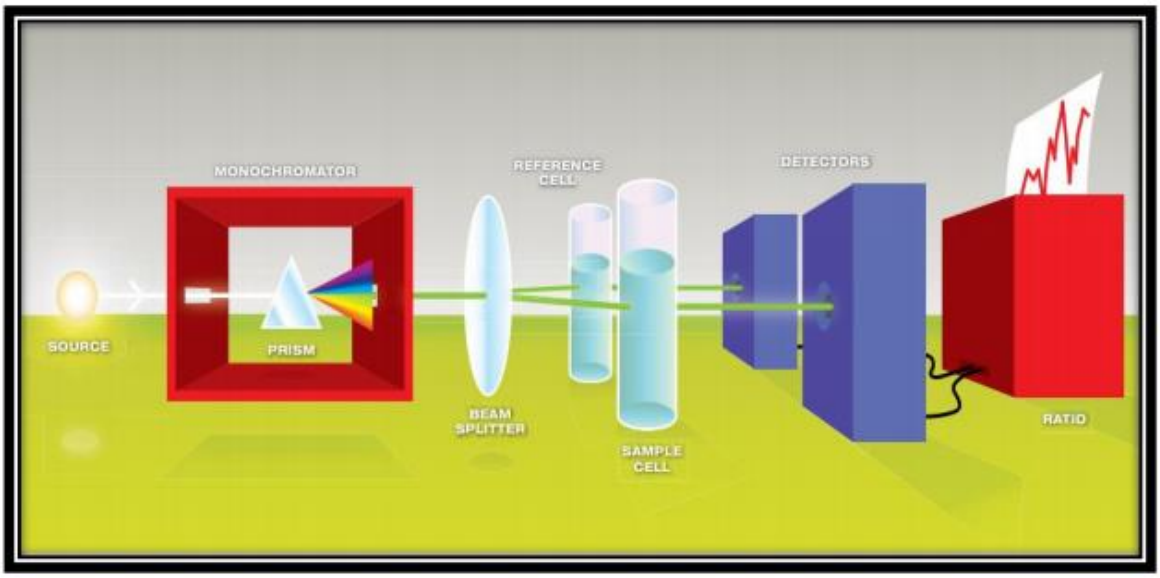

Figure 3.6 Schematic illustration of the UV-Spectrometer setup

3.5.3. Calculation of Optical bandgap

Tau plot is used for the measurement of the optical band gap calculation,

$$(\alpha h\upsilon)n \;=\; A\,(h\upsilon - E_g)$$

Where,

α = Absorbance

A= Proportionality constant

h= Planck's constant

E_g= Band gap energy

υ = Frequency of vibrations

n= Nature of optical transitions (n=2 direct allowed transition, n=1/2 indirect allowed transitions)

Chapter 04

Synthesis

This chapter is to explain all the experimental procedure that has been followed for the synthesis of Ag-rGO using Eriochrome Black T and Methyl Orange as reducing and stabilizing agent.

4.1. Experimental Procedure For synthesis of Ag-rGO: EBT Nanocomposite

To reduce silver nanoparticles using Eriochrome Black T as a dye, following steps were followed[104]:

1. 1mM solution of $AgNO_3$ was derived by mixing 13.61mg of silver nitrate in 80 milliliter of distilled water.
2. 0.2mM solution of Eriochrome black T was derived by mixing 7.45mg of Eriochrome Black T in 80 milliliter of distilled water.
3. 1uM solution of Graphene oxide was derived by adding1.467mg of Graphene oxide in 80 milliliter of distilled water
4. The solution containing silver nitrate was added to the solution containing Eriochrome Black T
5. The mixture was stirred for 40 minutes at room temperature.
6. After 40 minutes, the solution containing Graphene Oxide was added to the mixture of silver nitrate and EBT solution.
7. The whole solution was then put on to sonication for 40 minutes to disperse the grapheme oxide sheets in the mixture.
8. The pH of solution was adjusted to 9 using sodium hydroxide which is basic in nature and acts as a reducing agent.
9. After 40 minutes of sonication, we acquire a resultant dark brownish colored solution that indicates the formation of silver nanoparticles.
10. The solution was then placed at room temperature for 24 hours without any agitation.
11. After 24 hours, the solution was then washed using filter tubes in centrifuge machine. The filter tubes consisted of 2 parts i.e., **Supernatant** (upper vial) and **Sediment** (lower vial.)

12. Free dye and water were thrown towards bottom (the sediment) and the supernatant was the composite of Ag-rGO[105]

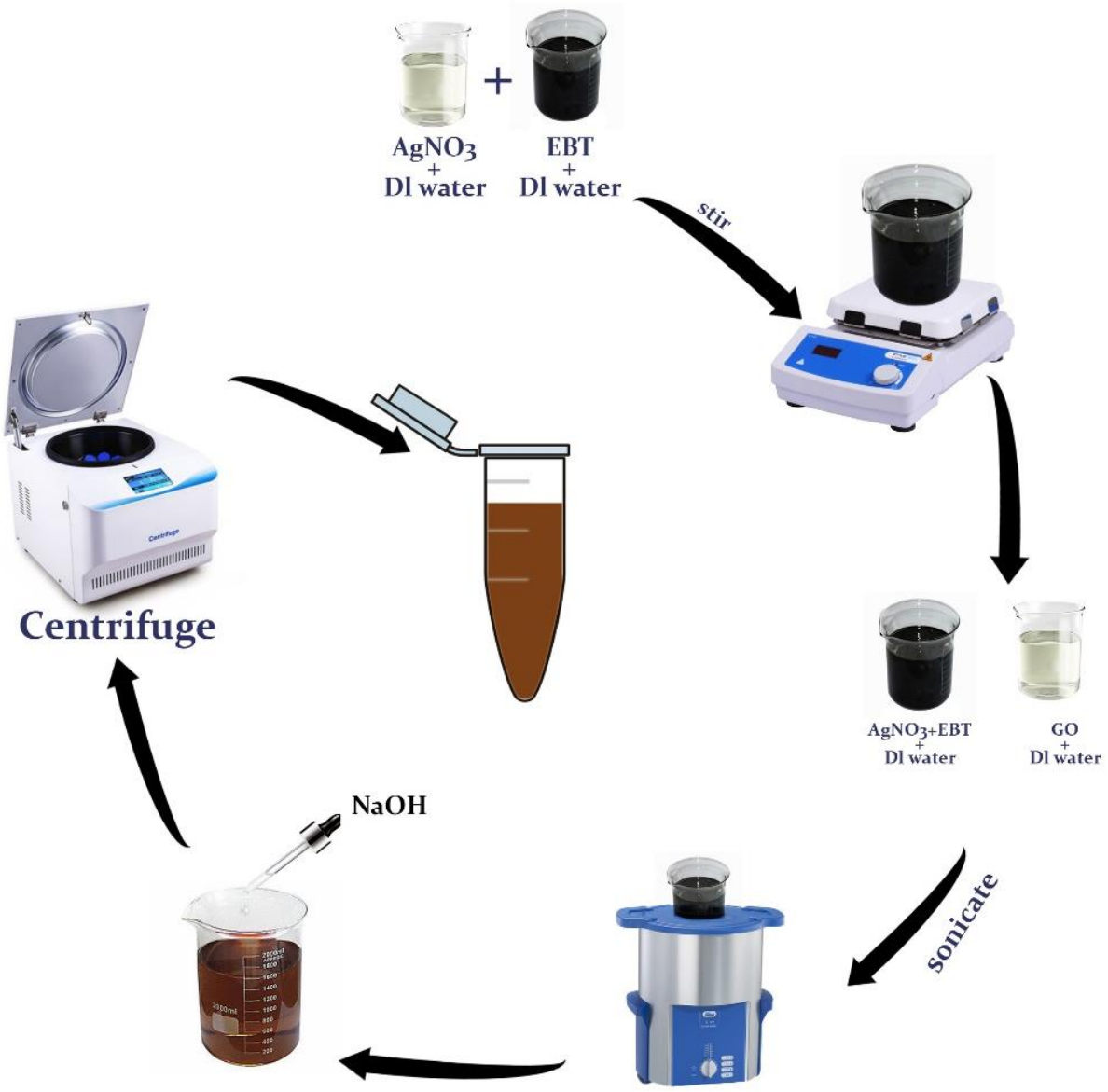

Figure 4.1 Synthesis using EBT dye as reducing agent

4.2. Experimental Procedure For synthesis of Ag-rGO: MO Nanocomposite

Following steps were followed for the synthesis of Ag-rGO using Methyl Orange as a dye[106].

1. 1mM solution of $AgNO_3$ was derived by mixing 13.61mg of silver nitrate in 80 milliliter of distilled water.
2. 0.2mM solution of Methyl Orange was derived by mixing 7.45mg of Methyl Orange in 80 milliliter of distilled water.
3. 1uM solution of Graphene oxide was derived by adding1.467mg of Graphene oxide in 80 milliliter of distilled water
4. The solution containing silver nitrate was added to the solution containing Methyl Orange.
5. The mixture was stirred for 40 minutes at room temperature.
6. After 40 minutes, the solution containing Graphene Oxide was added to the mixture of silver nitrate and EBT solution.
7. The whole solution was then put on to sonication for 80 minutes to disperse the grapheme oxide sheets in the mixture.
8. The pH of solution was adjusted to 9 using sodium hydroxide which is basic in nature and acts as a reducing agent.
9. After 40 minutes of sonication, we acquire a resultant dark brownish colored solution that indicates the formation of silver nanoparticles.
10. The solution was then placed at room temperature for 24 hours without any agitation.
11. After 24 hours, the solution was then washed using filter tubes in centrifuge machine.

12. Free dye and water was thrown towards bottom (the sediment) and the supernatant was the composite of Ag.[105]

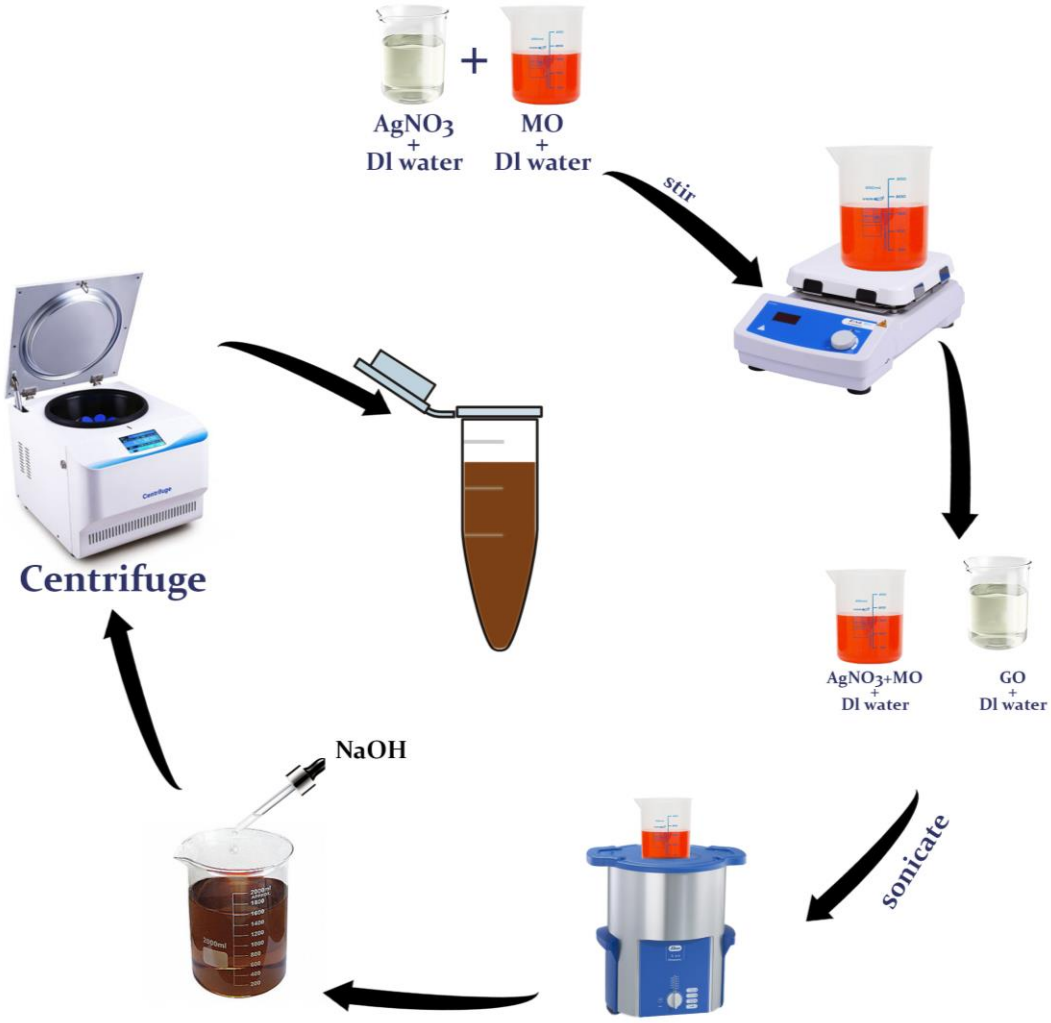

Figure 4.2 Synthesis2 using MO dye as reducing agent

Chapter 05

Results and Analysis

The synthesis of Ag-rGO composite has been counter tested using following techniques:

1. UV-Visible Spectroscopy
2. X-Ray Diffraction
3. Scanning Electron Microscopy
4. Energy Dispersive X-rays Spectroscopy
5. Fourier Transform Infrared Spectroscopy
6. Raman Spectroscopy

5.1. UV-Visible Spectroscopy

5.1.1. Ag-rGO: EBT

The presence of silver nanoparticles is verified from a peak at about 420-430 nm. The presence of rGO is evident from the peak at about 250-260 nm. At x-axis, we took wavelength in

nanometers and at y-axis, we have relative intensity that has arbitrary units.

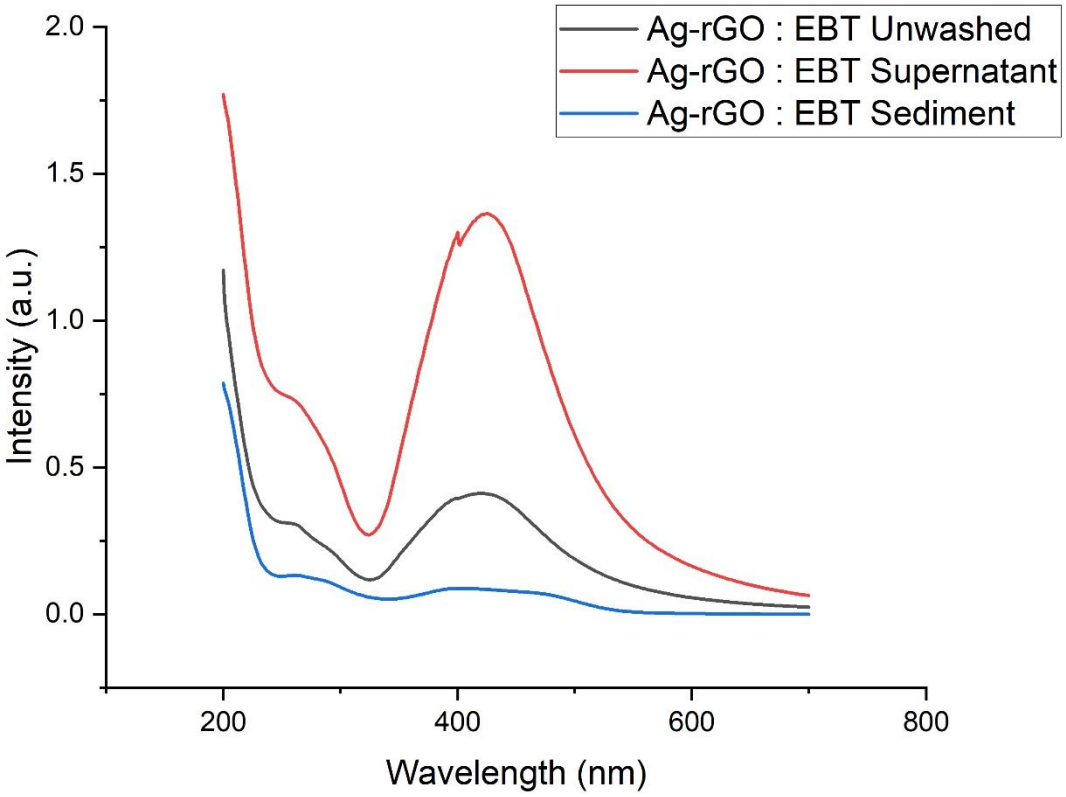

Figure 5.1 UV visible spectroscopy of Ag-rGO: EBT

In the above figure, we can see three spectra of our sample using Eriochrome Black T as a dye.

The black peak is the spectra just taken after the sonication without washing. We can see silver nanoparticles peak at a relatively lower intensity.

The red line shows the supernatant that was left in the upper vial of the filter tube after centrifugation. We can see a relatively higher magnitude of peaks for both Ag and rGO in this case.

At the bottom most, we have free EBT as our sediment. The peak of EBT is at about 460 nm.

5.1.2. Ag-rGO: MO

Methyl orange, being a stronger dye as compared to the Eriochrome Black T, we had to sonicate it for 40 more minutes than we did using Eriochrome Black T. However, the particles obtained

after the dispersion of graphene oxide in the sample containing methyl orange dye gave far better results than Eriochrome Black T.

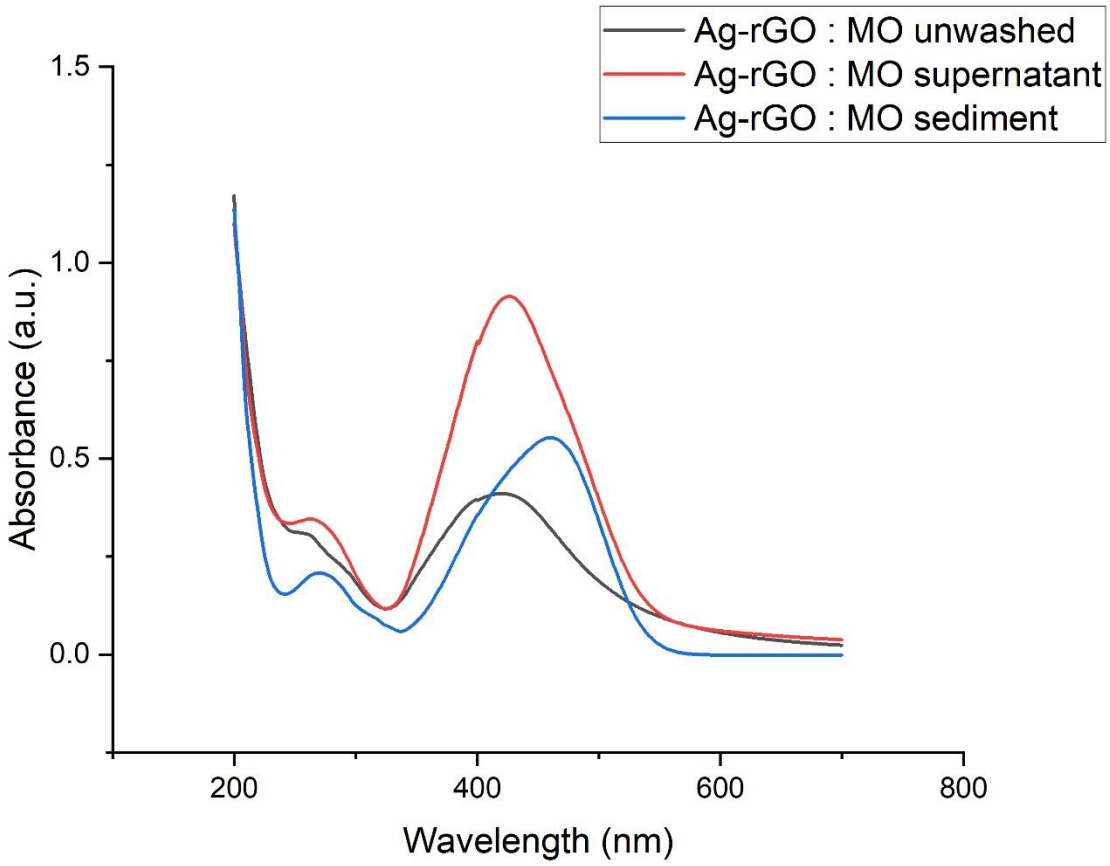

Figure 5.2 UV visible spectroscopy of Ag-rGO: MO

The black spectra show the situation of just after sonication without washing. We can see a relatively smaller peak for silver nanoparticles along with its broadening to the methyl orange dye that emerges at about 460 nm.

The red graph shows the supernatant in the upper vial of the filter tube. We can clearly see a higher magnitude peak for silver nanoparticles at about 420 nm. At about 250 nm, we can also see rGO peak.

The blue graph is nothing but the free dye present in the sediment vial. This is nothing but methyl orange in water.

5.2. X-Ray Diffraction

After depositing the supernatants obtained after filtration on a thin film, the samples were characterized by X-rays Diffraction technique. Relative intensity was calculated against Bragg's angle:

$$n\lambda = 2d \sin\theta$$

The miller indices were calculated using:

$$d_{hkl} = a / \sqrt{(h^2 + k^2 + l^2)}$$

5.2.1. Ag-rGO: EBT

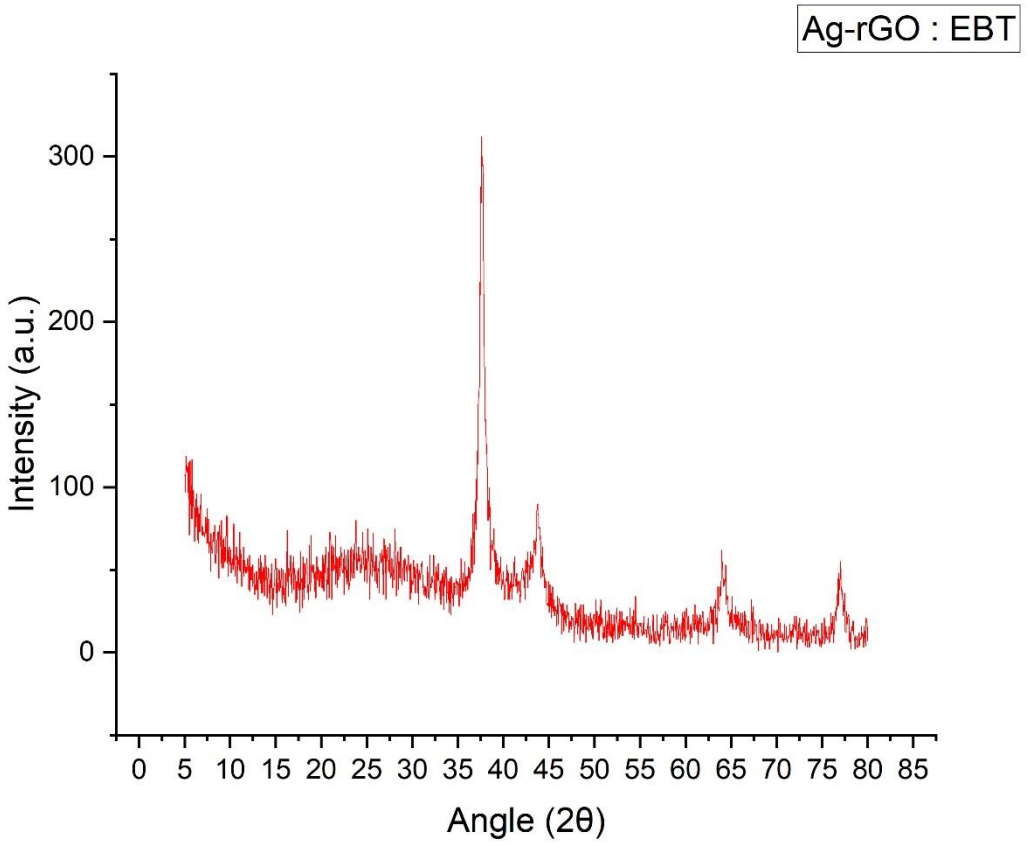

Figure 5.3 XRD results of Ag-rGO: EBT

In above sample, we have used Eriochrome Black T as our reducing and stabilizing dye. Presence of silver nanoparticles in the sample is confirmed from the peaks at 38.19°, 44.27°, 64.81°, 77.45° with miller indices (111), (200), (220) and (311) respectively.

The broad peak between 2θ = 20-30° indicates the presence of rGO in the sample.

5.2.2. Ag-rGO: MO

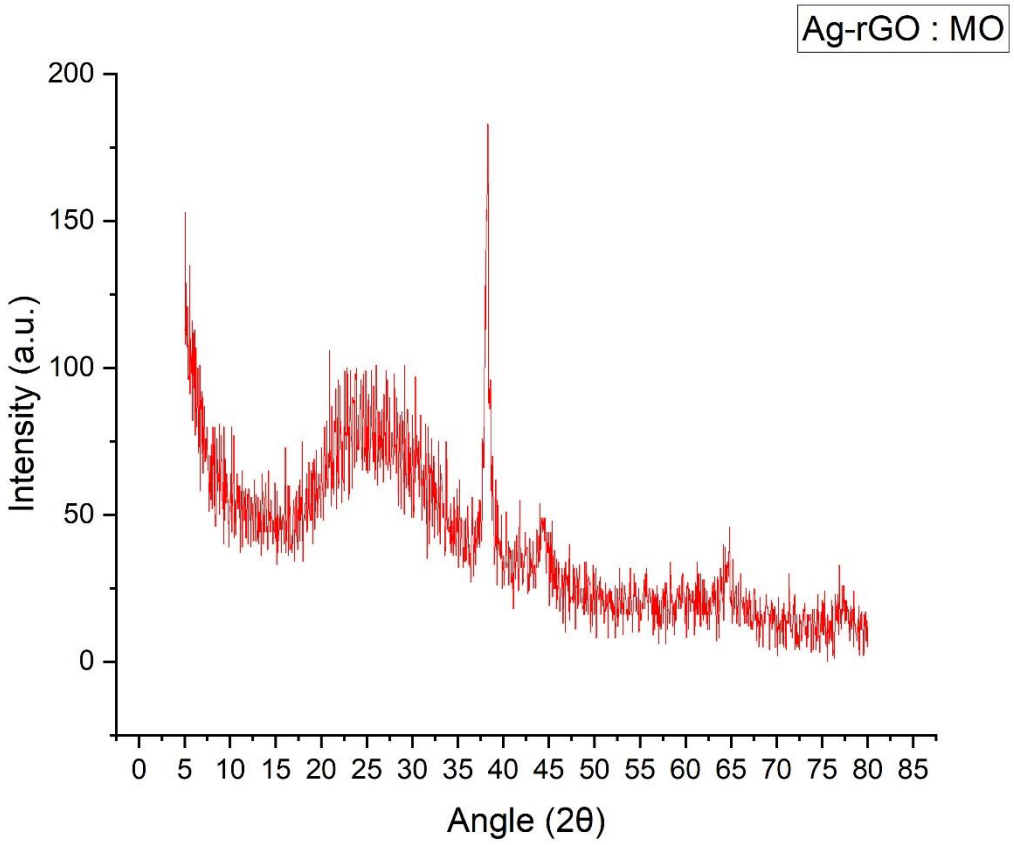

Figure 5.4 XRD results of Ag-rGO: MO

Methyl orange was used as a dye in the above sample.

Between 20 and 30 degrees, we can see a broad peak that confirms the presence of reduced graphene oxide.

The peaks at 38.32º, 44.25º, 64.87º, 77.51º having miller indices (111), (200), (220) and (311) respectively, are of silver nanoparticles.

5.2.3. Graphene Oxide

We have used Graphene oxide for the reduction of silver nanoparticles. The XRD of graphene oxide sheet is given below:

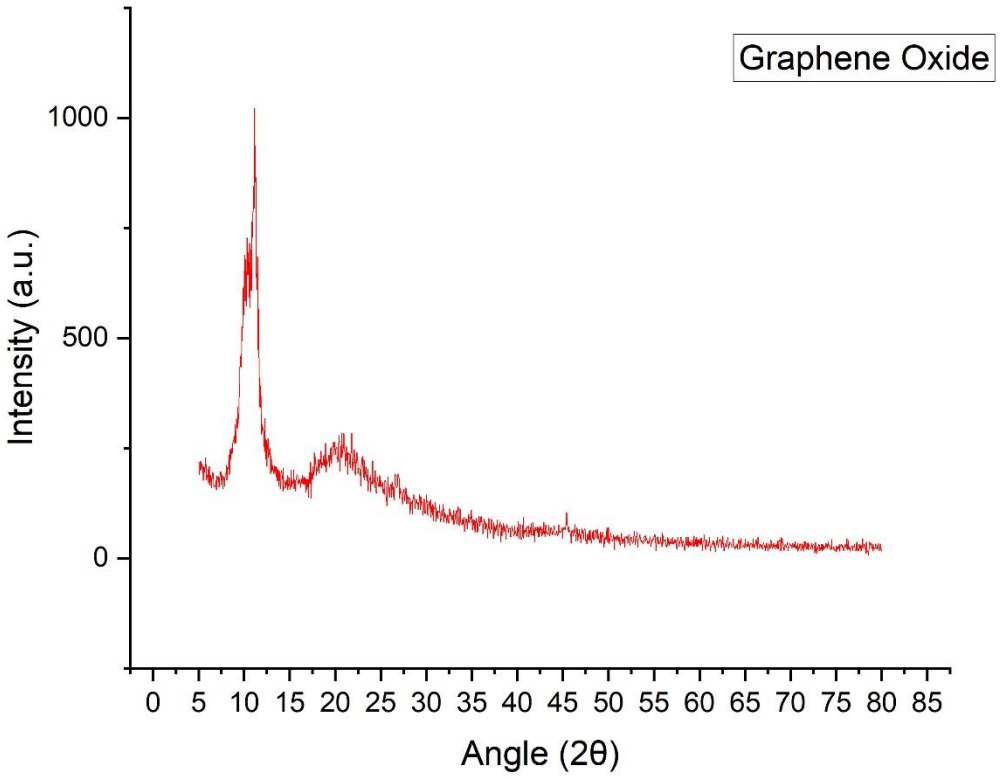

Figure 5.5 XRD results of graphene oxide

At 10.48^{o,} we can see a peak that confirms the structure of graphene oxide. The miller indices for which is (001). We can also see a broad hump between 15 and 25 that shows the already reduced behavior for graphene oxide.

5.3. Scanning Electron Microscopy

For surface analysis and imaging, the samples went under scanning electron microscope. In the microscope, silver nanoparticles with reduced graphene oxide sheets can be clearly seen. Using the secondary and backscattered electrons of scanning electron microscope, we have obtained some images of our samples that are represented below.

5.3.1. Ag-rGO: EBT

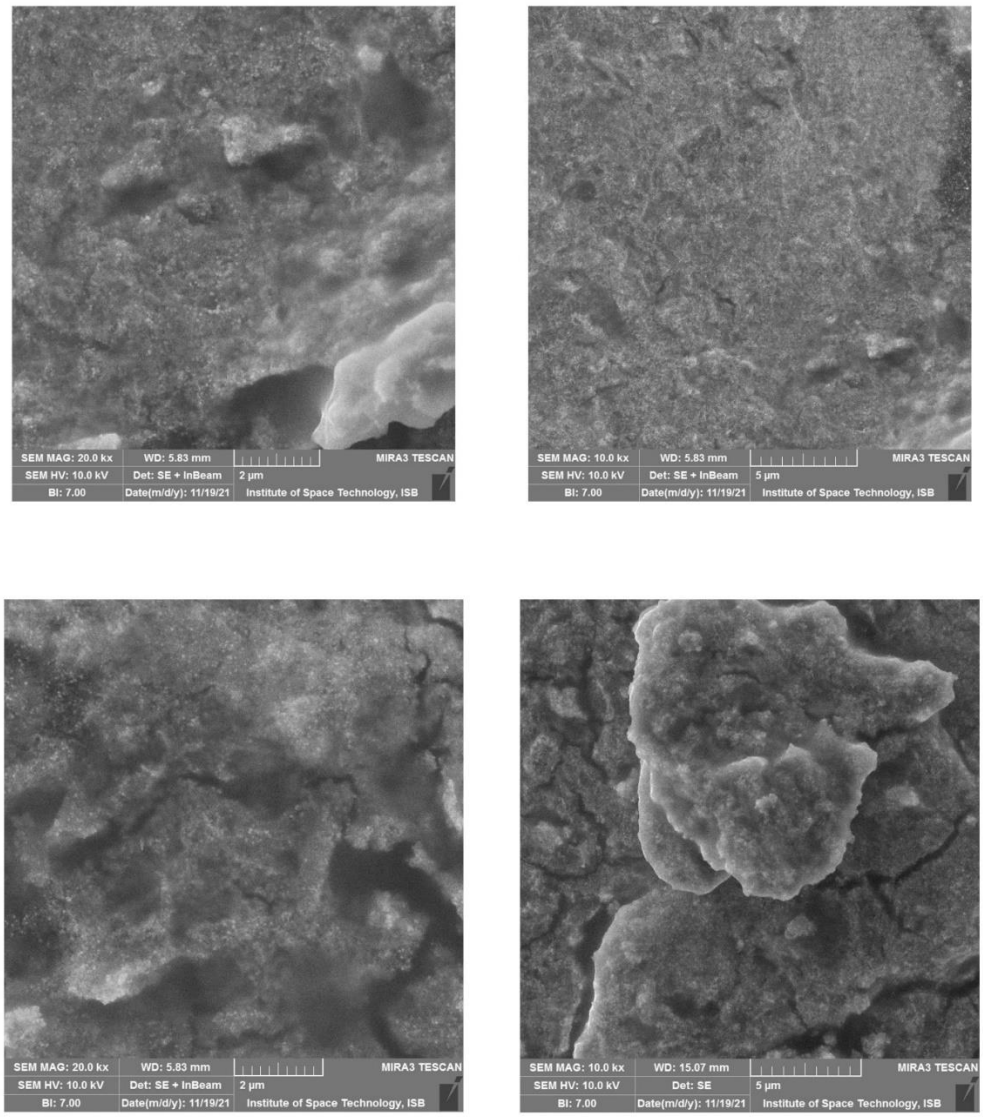

Figure 5.6 SEM results of Ag-rGO: EBT

In the above images, we can clearly see reduced graphene oxide sheets and silver nanoparticles topped upon them. The scales are taken to be 2 µm and 5 µm. The elemental analysis will also be presented in the next section that conform to the presence of silver and graphene elements (C, O, H).

5.3.2. Ag-rGO: MO

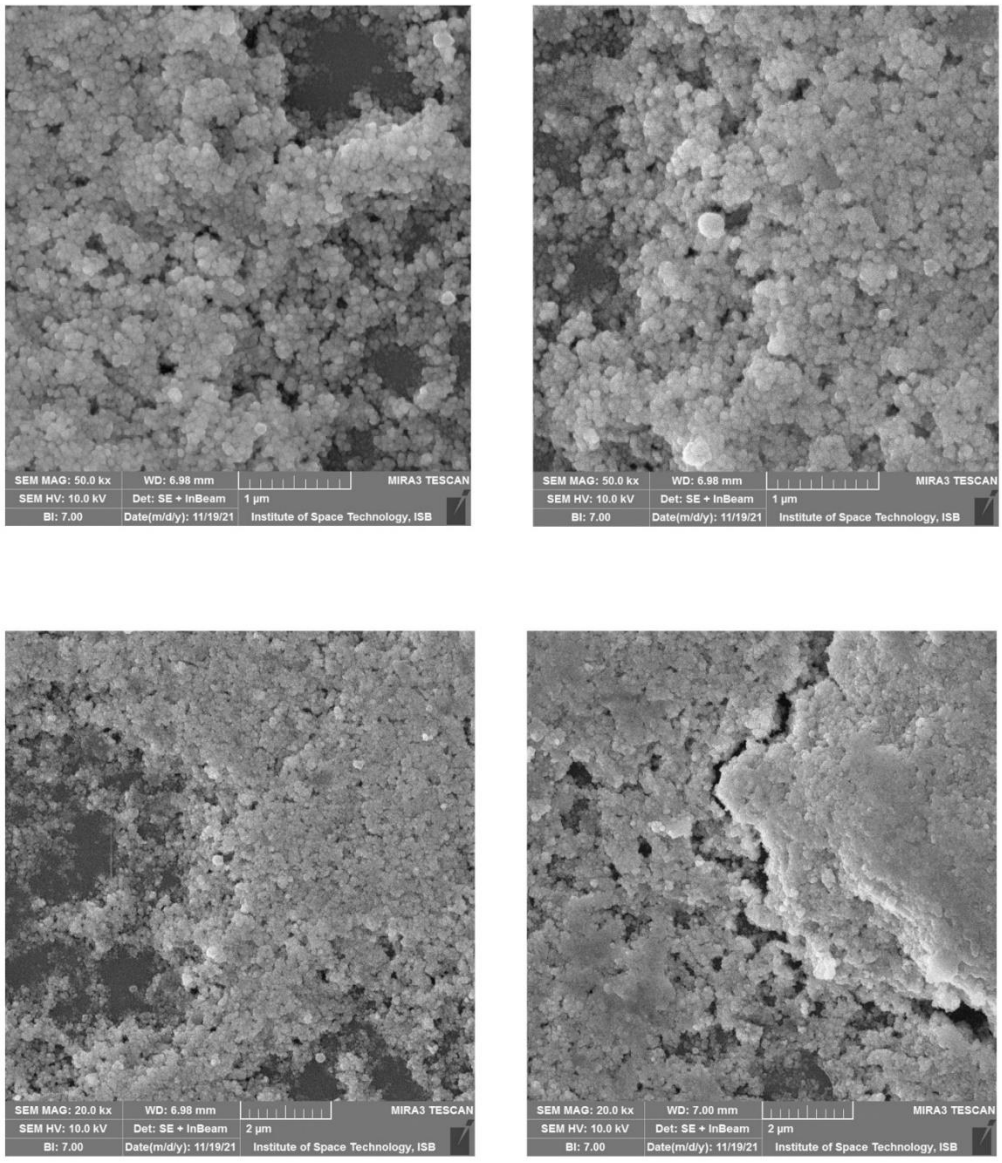

Figure 5.7 SEM results of Ag-rGO: MO

In the case of using methyl orange as reducing agent, we can see a much better performance in the production of silver nanoparticles. The particles can be clearly viewed from different perspectives.

Images are taken at 1 µm and 2 µm respectively. The resolution is even better as compared to the previous images.

5.3.3. Graphene Oxide

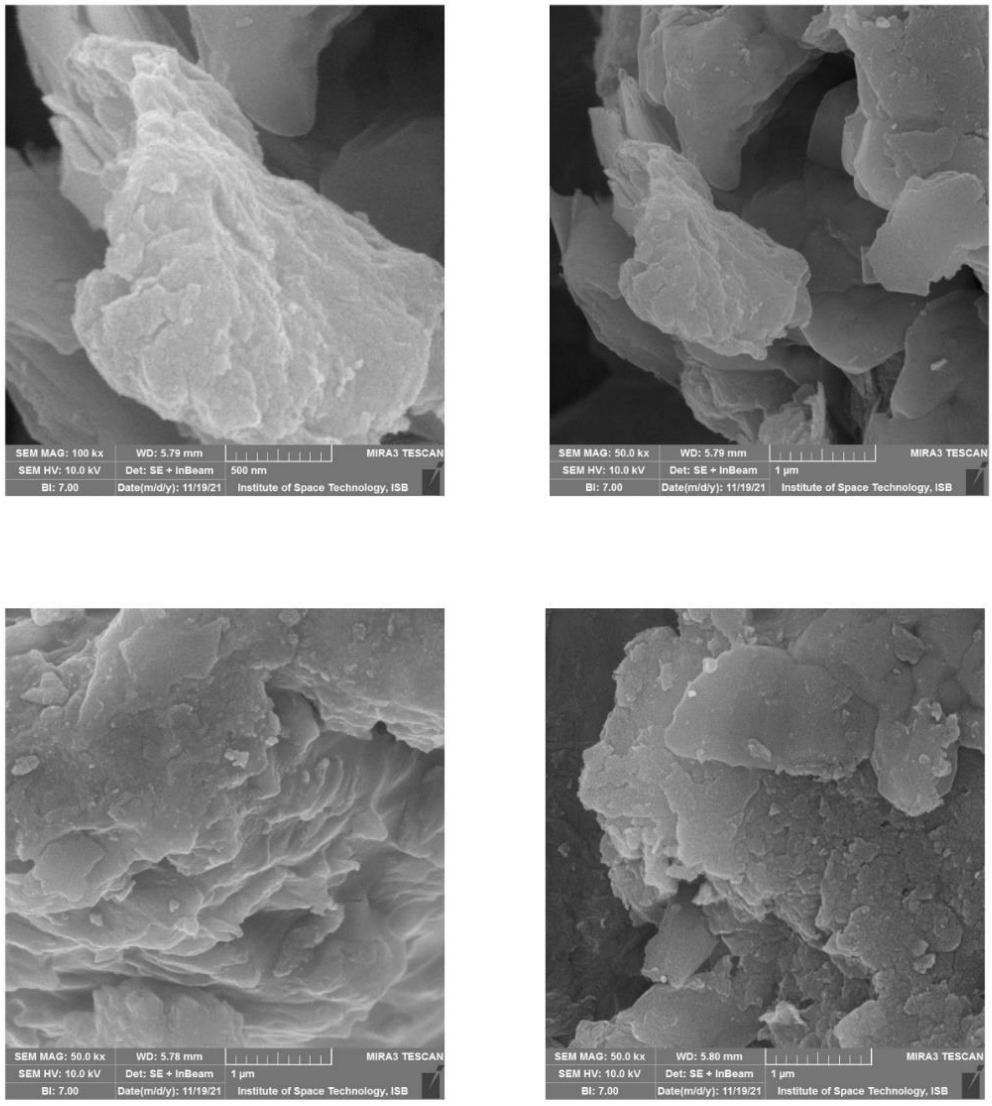

Figure 5.8 SEM results of graphene oxide

Above are the images for graphene oxide which was then reduced to rGO. The rolled leaves images confirm the structure of graphene oxides. We can also see sheets of graphene oxide here.

These images were taken at scales of 500 nm and 1 µm.

5.4. Energy Dispersive X-Rays Spectroscopy

For elemental composition and atomic weight percentage of each element in the sample, we have used the X-rays electrons generated during SEM.

5.4.1. Ag-rGO: EBT

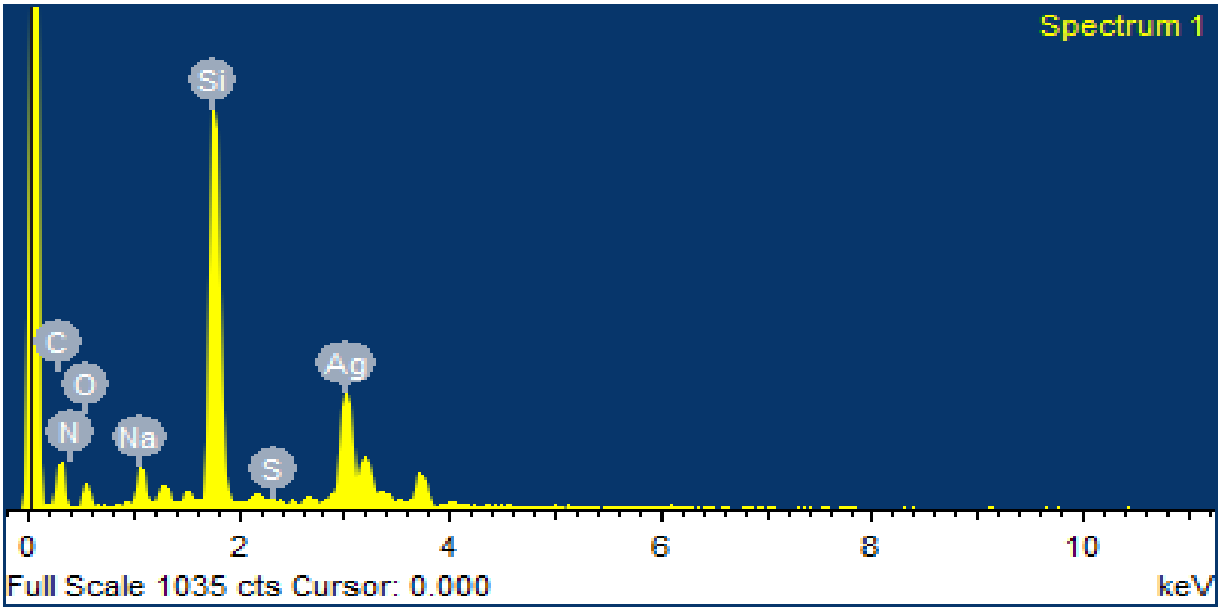

Figure 5.9 EDS results of Ag-rGO: EBT

Above are the spectra generated by EDS spectroscopy. We can see peaks of different elements with different concentrations and atomic weight percentage

Table 2 Elemental composition of Ag-rGO: EBT

Element	Weight%	Atomic%
C	26.06	47.64
N	2.89	4.53
O	13.00	17.85
Na	3.89	3.72
Si	26.20	20.48
S	0.17	0.12
Ag	27.79	5.66
Totals	100.00	

Carbon and Oxygen elements are present due to graphene oxide. Nitrogen and sodium are the elements of EBT dye. We can see silicon that is due to the glass substrate. Sulphur is an impurity.

A large volume of Ag can also be seen.

5.4.2. Ag-rGO: MO

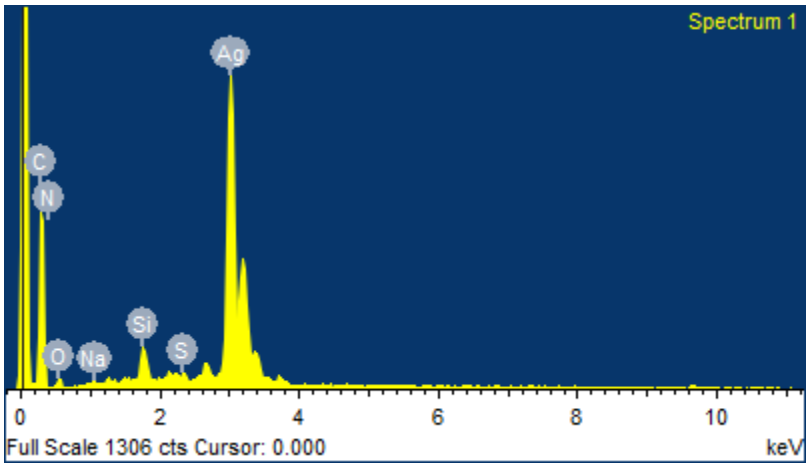

Figure 5.10 EDS results of Ag-rGO: MO

Table 3 Elemental composition of Ag-rGO: MO

Element	Weight%	Atomic%
C	29.07	67.20
N	4.68	9.27
O	3.10	5.39
Na	0.12	0.14
Si	2.17	2.15
S	0.32	0.28
Ag	60.54	15.58
Totals	100.00	

Carbon and Oxygen arise from the presence of graphene oxide. Nitrogen and sodium are due to the presence of methyl orange dye. Silicon arises due to glass substrate. Sulphur is an impurity. Silver element can also be seen in the elemental analysis that confirms silver nanoparticles in the structure.

5.4.3. Graphene Oxide

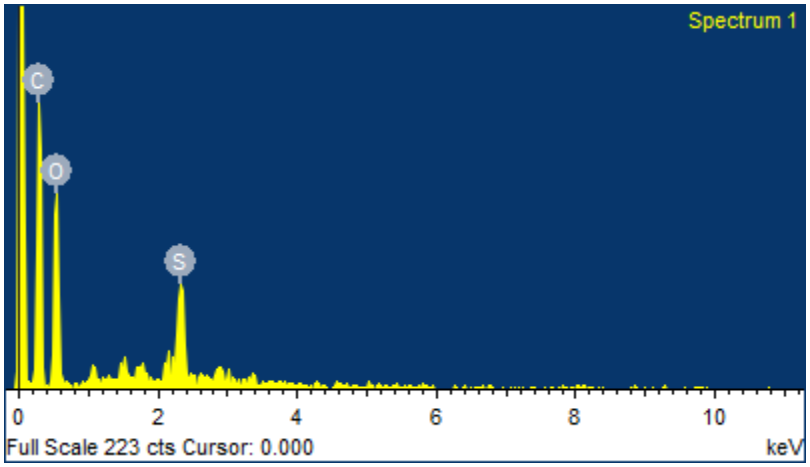

Figure 5.11 EDS results of graphene oxide

Table 4 Elemental composition of graphene oxide

Element	Weight%	Atomic%
C	50.56	58.71
O	45.29	39.48
S	4.15	1.80
Totals	100.00	

Above is the EDS of graphene oxide which shows carbon and oxygen with a massive volume and some traces of sulfur as an impurity.

5.5. Fourier Transform Infrared Spectroscopy

We have obtained the information of functional groups present in the sample with the help of FTIR spectroscopy. O-H, C=C, -C-H and C ≡ N bonds can be seen in both Ag-rGO : EBT and Ag-rGO : MO samples.

5.5.1. Ag-rGO: EBT

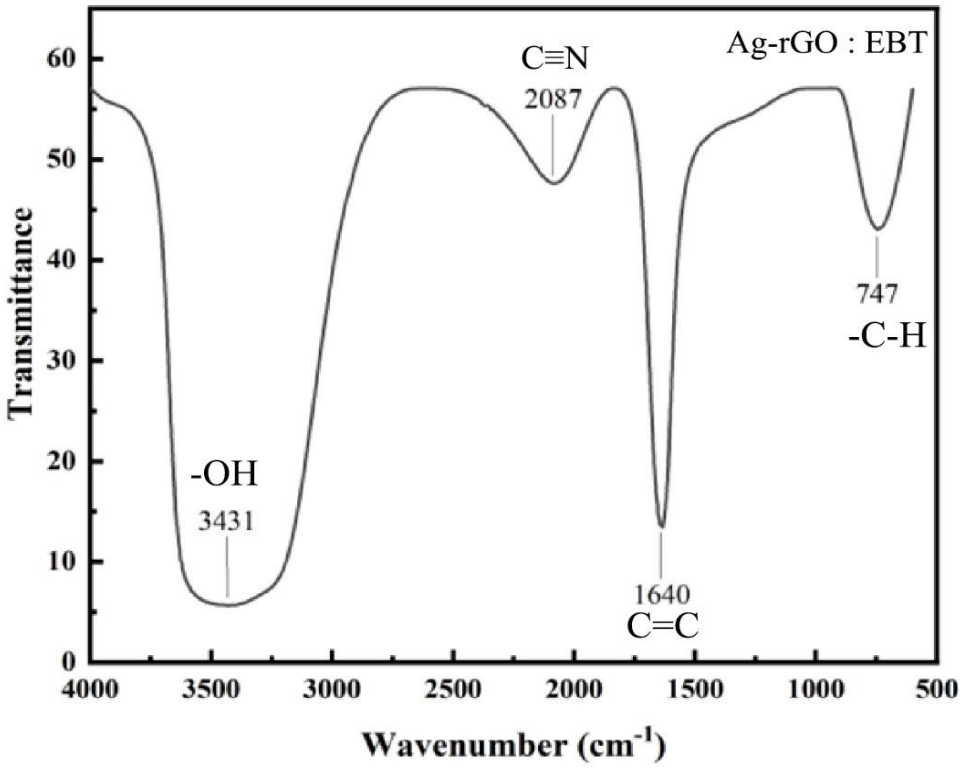

Figure 5.12 FTIR results of Ag-rGO: EBT

Transmittance has been calculated against wavenumber. -OH bond indicates the presence of graphene oxide.

5.5.2. Ag-GO: MO

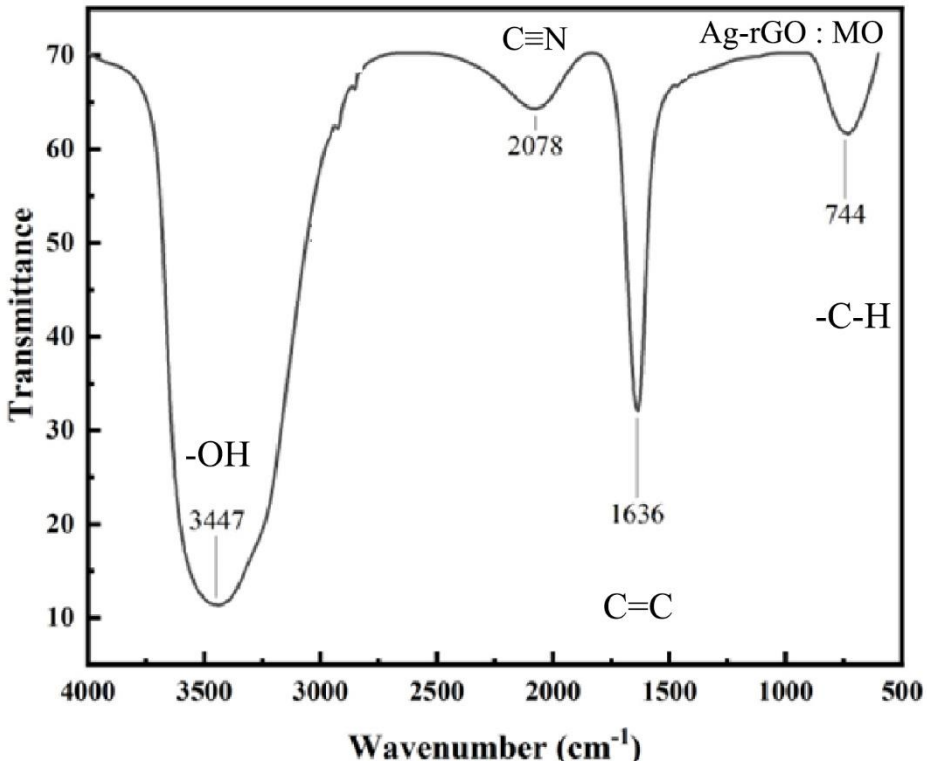

Figure 5.13 FTIR results of Ag-GO: MO

Like the previous results, we can see -OH, C=C, C≡N and -C-H functional groups.

The transmittance has been calculated against wavenumber.

5.6. Raman Spectroscopy

The vibrational modes of molecules in the sample have been calculated using Raman spectroscopy. The D and G bands give the in-plane and out of plane vibrations of sp^2 bonded carbon atoms respectively.

5.6.1. Ag-rGO: EBT

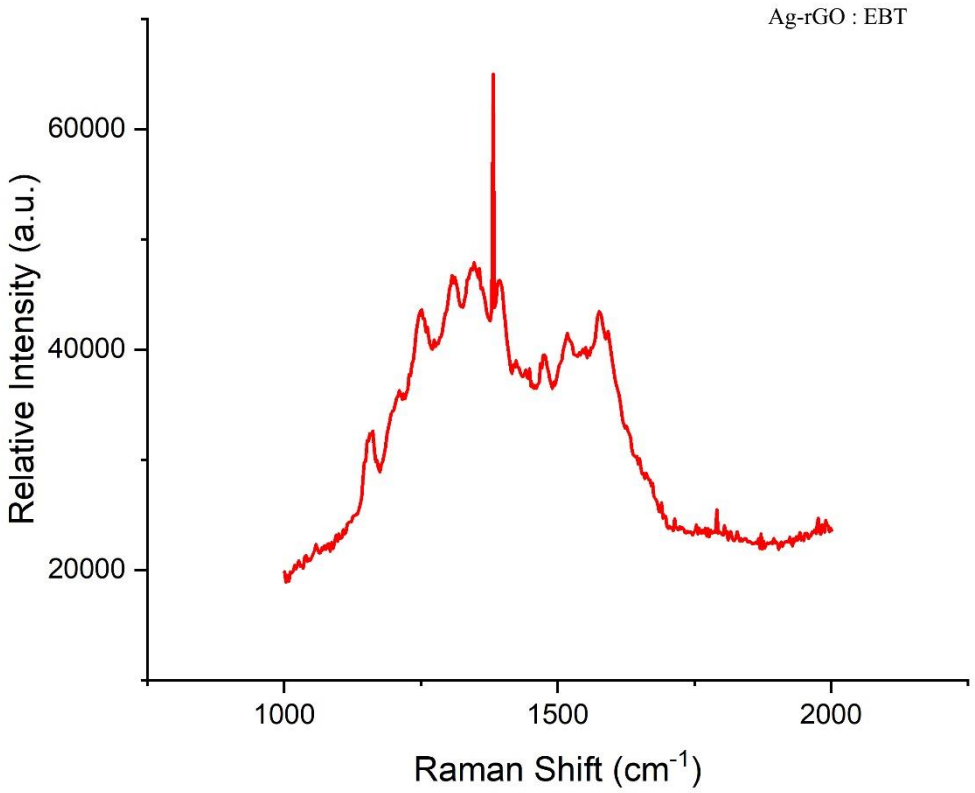

Figure 5.14 Raman spectroscopy results of Ag-rGO: EBT

In the above spectra, we can observe a D-band at about 1350 cm^{-1} and G-band at 1580 cm^{-1}. These bands are calculated using Stokes and Anti-Stokes scattered Raman rays.

5.6.2. Ag-rGO: MO

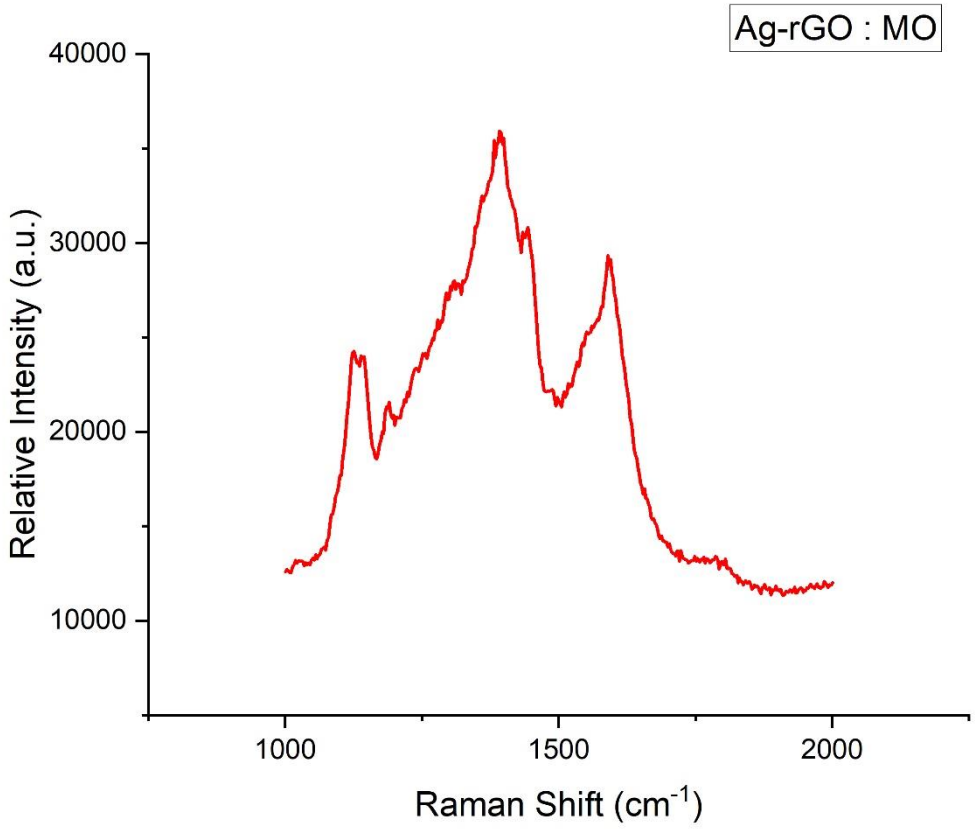

Figure 5.15 Raman spectroscopy results of Ag-rGO: MO

The above spectra show D band at 1210 cm^{-1} and G-band at 1540 cm^{-1}. The intensity taken is relative. The readings were taken in dark room to avoid any photon interaction while performing the spectroscopy.

Chapter 06

Applications

Silver nanoparticles find a wind range of applications. They give a strong response for photocatalysis dye degradation which can be used for water purification. Ag nanoparticles, when exposed to bacteria, exhibit a wide inhibition zone so that they can also be used as antibacterial agents. We have extended our research to conform the applications of silver nanoparticles and their composite with reduced graphene oxide.

6.1. Photocatalytic Dye Degradation:

Following steps have been followed for the study of dye degradation of silver nanoparticles

1. Solutions containing Ag-rGO: EBT and Ag-rGO: MO were added to 1 ppm solution of methylene blue (in separate beakers) which is also an azo dye.
2. The mixture was stirred inside the photochemical reactor and a lamp was shined upon the samples
3. Samples were extracted out after intervals of 10 minutes for a total of 50 minutes
4. Obtained samples were centrifuged so the sediment settles down at the bottom and supernatant remains at top.
5. Photocatalytic dye degradation has been verified from UV-visible spectroscopy

6.1.1. Ag-rGO: EBT @ Methylene Blue:

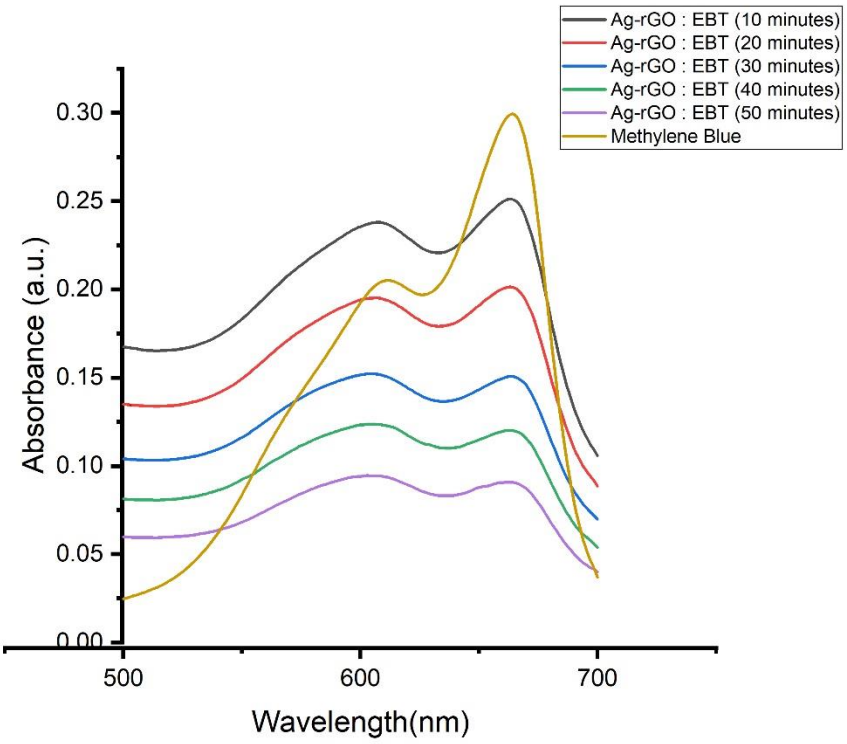

Figure 5.16 Photocatalytic dye degradation using Methylene Blue as dye

Methylene blue peak is generally observed at 560 nm. As we can see in the above graph, after each interval of 10 minutes, we can see a constant decline in the relative absorption of methylene blue which means that our sample is degrading the dye efficiently.

The degradation efficiency has been calculated using the following formula:

$$D\% = \frac{Ao - A}{Ao} \times 100\%$$

After 50 minutes, the degradation efficiency turns out to be ~ 80% that evidences a strong degradation quality present in the sample.

6.1.2. Ag-rGO: MO @ Methylene Blue:

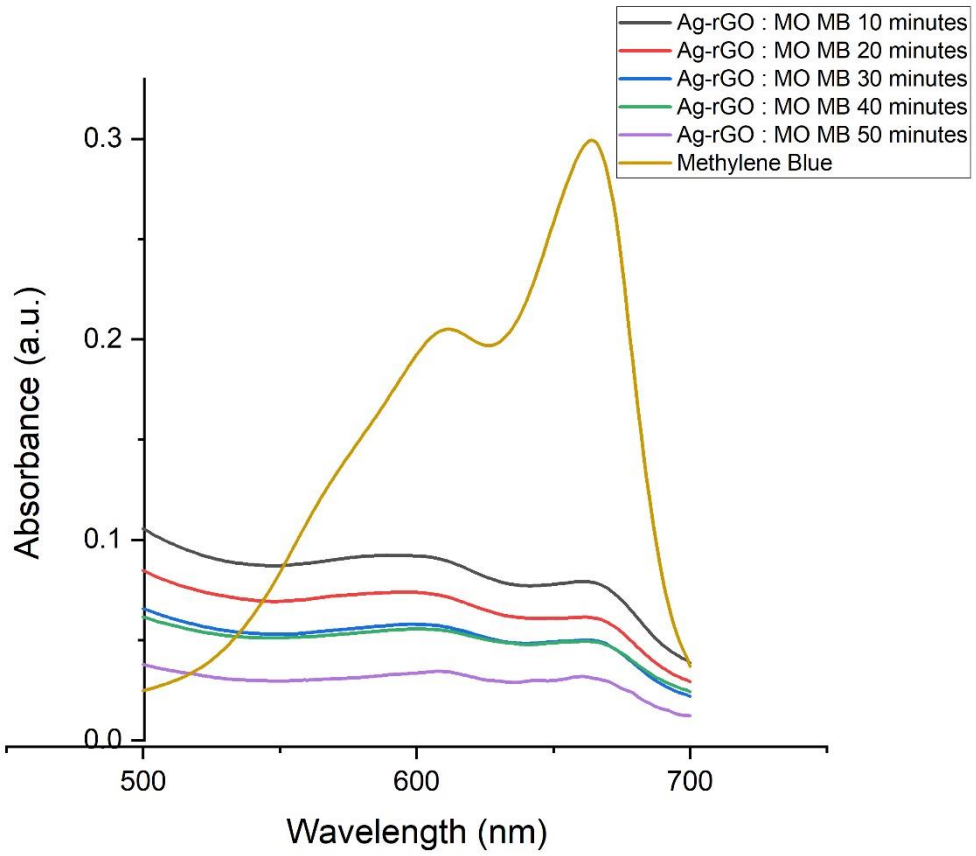

Figure 5.17 Photocatalytic dye degradation using Methylene Blue as dye

Like the previous results, here we can also see a strong degradation for the externally introduced methylene blue dye. The degradation here shows even better results than the previous ones.

Using the same formula, we can calculate the degradation efficiency of this sample which turns out to be ~ 86%

The above data suggests that our composite can be used for water purification due to its strong degradation properties under the presence of light.

6.2. Antibacterial Activity

We have also studied the antibacterial properties exhibited by our samples as silver is a strong antibacterial agent against different strains of bacteria

The process is as follows:

1. At a constant optical density, bacteria culture is grown on a petri dish.
2. We have tested our samples on two different strains. One is bacillus subtilis (a gram-positive bacteria) and the other one is pseudomonas aeruginosa (a gram-negative bacteria)
3. At 5 different relative concentrations, results have been taken out.
4. The minimum inhibition zone for both strains was about 7mm, and the maximum was 9mm.

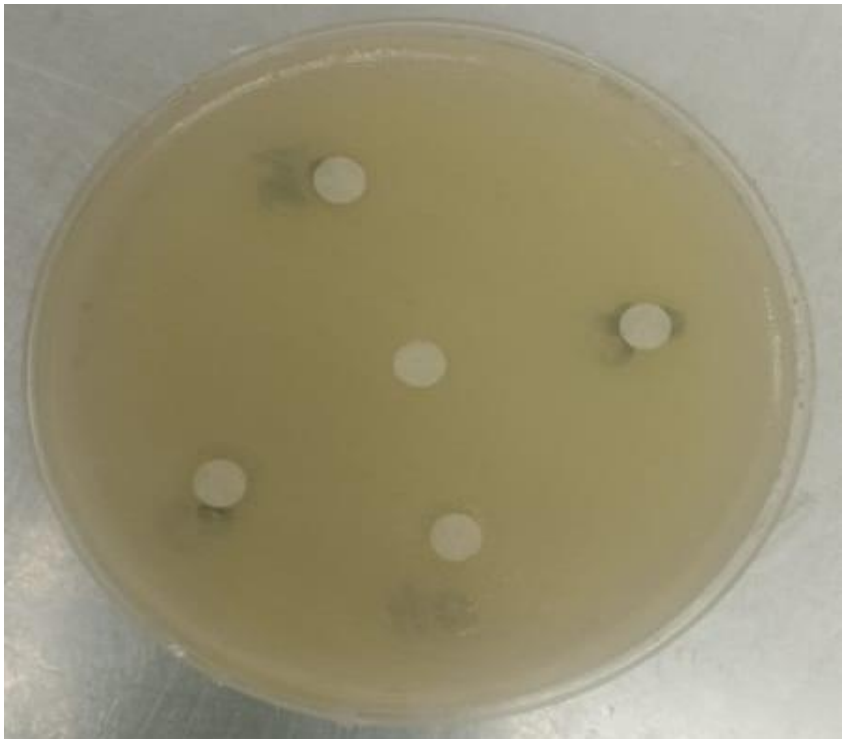

Figure 5.18 Visualization of inhibition zone spread by each concentration of the sample

The results obtained were as follows:

Table 5 Inhibition zone generated by relative concentrations of Ag-rGO: EBT

Ag-rGO: EBT Relative Concentrations	**Inhibition zone (mm)**
100%	9
75%	9
50%	8
25%	7
10%	7

Table 6 Inhibition zone generated by relative concentrations of Ag-rGO :MO

Ag-GO-MO (Relative concentration)	**Inhibition Zone (mm)**
100%	9
75%	8
50%	7
25%	7
10%	7

Chapter 07

Achievements and Conclusions

Achievements

As a conclusion of this research, a novel approach has been followed for the synthesis of silver nanoparticles and its composite with rGO. The synthesis is optimized to be easy, safe and less expensive. Azo dyes (Eriochrome Black T and Methyl Orange) played a vital role in reducing silver nanoparticles. After synthesis, the dyes get capped on the surface of the samples.

Using silver salt and graphene oxide with Eriochrome Black T at pH 9, the composite Ag-rGO: Azo Dye was successfully synthesized in a well stabilized condition. Dye degradation and antibacterial activities have been proved as applications to Ag-rGO composite.

Conclusions

1. Silver nanoparticles were extracted from silver nitrate using Eriochrome Black T and Methyl orange as reducing agents.
2. Graphene oxide was sonicated with the mixture containing silver nitrate and dye to disperse the graphene oxide sheets into the solution and to form a composite of graphene oxide with silver nanoparticles
3. The elemental analysis, surface morphology, optical properties, crystal structure, functional groups, and vibrational modes of Ag-rGO composite were studied from UV visible spectroscopy, X-Ray Diffraction, Scanning Electron Microscopy, Energy Dispersive X-Rays, Raman Spectroscopy and Fourier Transform Infrared Spectroscopy.
4. Degradation efficiency percentage calculation proved a significant degradation of the methylene blue dye.
5. A strong response against gram-positive and gram-negative strains of bacteria has been observed from the formation of inhibition zone against the strains.

References

1. David L. Andrews, Gregory D. Scholes and Gary P. Wiederrecht: Comprehensive Nanoscience and Technology (2011)

2. Teipel U. Energetic materials: particle processing and characterization. Published online 2005:621. 3. Campos-Cuerva C, Zieba M, Sebastian V, et al. Screen-printed nanoparticles as anti-counterfeiting tags. *Nanotechnology*. 2016;27(9). doi:10.1088/0957-4484/27/9/095702

4. Klapötke TM. Chemistry of high-energy materials. :257.

5. Foltynowicz Z, Czajka B, Maranda A, Wachowski L. Aspects of nanomaterials for civil and military applications. Part 2. Their use and concerns arising from their release into the natural environment. *Materiały Wysokoenergetyczne*. 2020; T. 12(1)(1):17-36. doi:10.22211/MATWYS/0158E.

6. Foundations of Nanotechnology, Volume Two: Nanoelements Formation and ... - Sabu Thomas, Saeedeh Rafiei, Shima Maghsoodlou, Arezo Afzali 7. Habiba K, Makarov VI, Weiner BR. Fabrication of Nanomaterials by Pulsed Laser Synthesis Enzymatic catalysis: Quantum theory and Quantum Coherence View project Development of multifunctional radiosensitizers to enhance radiotherapy in colorectal cancer View project. doi:10.13140/RG.2.2.16446.28483

8. Zhen Guo, Li: Fundamentals and Applications of Nanomaterials August 2019 DOI:10.1201/9780429425660-4

9. Gleiter H. Nanostructured materials: basic concepts and microstructure. *Acta Materialia*. 2000;48(1):1-29. doi:10.1016/S1359-6454(99)00285-2

10. Khan FA. Nanomaterials: Types, classifications, and sources. *Applications of Nanomaterials in Human Health*. Published online January 1, 2020:1-13. doi:10.1007/978-981-15-4802-4_1/COVER/

11. Pokropivny V v., Skorokhod V v. Classification of nanostructures by dimensionality and concept of surface forms engineering in nanomaterial science. *Materials Science and Engineering: C*. 2007;27(5-8):990-993. doi: 10.1016/J.MSEC.2006.09.023

12. Maciej Serda. Synteza i aktywność biologiczna nowych analogów tiosemikarbazonowych chelatorów żelaza. G. Balint, Antala B, Carty C, Mabieme JMA, Amar IB, Kaplanova A, eds. *Uniwersytet śląski*. Published online 2013:343-354. doi: 10.2/JQUERY.MIN.JS

13. Wang Z, Hu T, Liang R, Wei M. Application of Zero-Dimensional Nanomaterials in Biosensing. *Frontiers in Chemistry*. 2020; 8:320. doi:10.3389/FCHEM.2020.00320/BIBTEX

14. Zhao Y, Hong H, Gong Q, Ji L. 1D nanomaterials: Synthesis, properties, and applications. *Journal of Nanomaterials*. 2013;2013. doi:10.1155/2013/101836

15. Ji L, Zou X, Hsu HY, et al. Two-dimensional materials as photoelectrodes in water reduction devices for energy applications. *Emerging 2D Materials and Devices for the Internet of Things*. Published online 2020:165-179. doi:10.1016/B978-0-12-818386-1.00007-2

16. Ayinla Tobi: What is/are the major difference(s) between 0D, 1D, 2D and 3D nano carbonaceous materials (2018)

17. Yurkov GY, Fionov AS, Koksharov YA, Koleso V v., Gubin SP. Electrical and magnetic properties of nanomaterials containing iron or cobalt nanoparticles. *Inorganic Materials 2007 43:8*. 2007;43(8):834-844. doi:10.1134/S0020168507080055

18. Bharmoria P, Healthcare SVN for, and E, 2019 undefined. Optical applications of nanomaterials. *Springer*. 2019; 118:1-29. doi:10.1007/978-981-13-9833-9_1

19. Zhang JZ, Noguez C. Plasmonic optical properties and applications of metal nanostructures. *Plasmonics*. 2008;3(4):127-150. doi:10.1007/S11468-008-9066-Y

20. Gatoo MA, Naseem S, Arfat MY, Mahmood Dar A, Qasim K, Zubair S. Physicochemical properties of nanomaterials: Implication in associated toxic manifestations. *BioMed Research International*. 2014;2014. doi:10.1155/2014/498420

21. Mody V v., Siwale R, Singh A, Mody HR. Introduction to metallic nanoparticles. *Journal of Pharmacy and Bioallied Sciences*. 2010;2(4):282. doi:10.4103/0975-7406.72127

22. Gade A, Ingle A, Whiteley C, Rai M. Mycogenic metal nanoparticles: Progress and applications. *Biotechnology Letters*. 2010;32(5):593-600. doi:10.1007/S10529-009-0197-9/TABLES/2

23. Panigrahi S, Kundu S, Ghosh SK, Nath S, Pal T. General method of synthesis for metal nanoparticles. *Journal of Nanoparticle Research 2004 6:4*. 2004;6(4):411-414. doi:10.1007/S11051-004-6575-2

24. Fytianos G, Rahdar A, Kyzas GZ. Nanomaterials in Cosmetics: Recent Updates. *Nanomaterials 2020, Vol 10, Page 979*. 2020;10(5):979. doi:10.3390/NANO10050979

25. Harifi T, Montazer M. A review on textile sonoprocessing: A special focus on sonosynthesis of nanomaterials on textile substrates. *Ultrasonics Sonochemistry*. 2015; 23:1-10. doi: 10.1016/J.ULTSONCH.2014.08.022

26. Hu T, Mei X, Wang Y, Weng X, Liang R, Wei M. Two-dimensional nanomaterials: fascinating materials in biomedical field. *Science Bulletin*. 2019;64(22):1707-1727. doi: 10.1016/J.SCIB.2019.09.021

27. Bassett L. Quantum Mechanics with Applications to Nanotechnology and Information Science. *Physics Today*. 2014;67(7):50. doi:10.1063/PT.3.2451

28. Tan SG, Jalil MBA. Nanoscale physics and electronics. *Introduction to the Physics of Nanoelectronics*. Published online 2012:23-77. doi:10.1533/9780857095886.23

29. TAHMASEBI T, PIRAMANAYAGAM SN. NANOSCIENCE AND NANOTECHNOLOGY FOR MEMORY AND DATA STORAGE. *http://dx.doi.org/101142/S0219607711000705*. 2011;07(01):25-30. doi:10.1142/S0219607711000705

30. Guerra FD, Attia MF, Whitehead DC, Alexis F. Nanotechnology for Environmental Remediation:

Materials and Applications. *Molecules: A Journal of Synthetic Chemistry and Natural Product Chemistry*. 2018;23(7). doi:10.3390/MOLECULES23071760

31. Ghosh N, Das S, Biswas G, Haldar PK. Review on some metal oxide nanoparticles as effective adsorbent in wastewater treatment. *Water Science and Technology*. Published online May 16, 2022. doi:10.2166/WST.2022.153/88763/REVIEW-ON-SOME-METAL-OXIDE-NANOPARTICLES-AS

32. Tarafdar JC, Raliya R. Rapid, Low-Cost, and Ecofriendly Approach for Iron Nanoparticle Synthesis Using Aspergillus oryzae TFR9. *Journal of Nanoparticles*. 2013; 2013:1-4. doi:10.1155/2013/141274

33. Buzea C, Pacheco II, Robbie K. Nanomaterials, and nanoparticles: Sources and toxicity. *Biointerphases*. 2007;2(4):MR17-MR71. doi:10.1116/1.2815690

34. Lu H, Wang J, Stoller M, Wang T, Bao Y, Hao H. An Overview of Nanomaterials for Water and Wastewater Treatment. *Advances in Materials Science and Engineering*. 2016;2016. doi:10.1155/2016/4964828

35. Bazylewski P, Fanchini G. Graphene: Properties and Applications. *Comprehensive Nanoscience and Nanotechnology*. 2019;1-5:287-304. doi:10.1016/B978-0-12-803581-8.10416-3

36. Santosh K. Tiwaria, Sumanta Sahoob, Nannan,Wanga, Andrzej Huczko : Graphene research and their outputs: Status and prospect Volume 5, Issue 1, March 2020, Pages 10-29 37. Du M, Wu Y, Hao X. A facile chemical exfoliation method to obtain large size boron nitride nanosheets. *CrystEngComm*. 2013;15(9):1782-1786. doi:10.1039/C2CE26446C

38. Habte AT, Ayele DW, Hu M. Synthesis and Characterization of Reduced Graphene Oxide (rGO) Started from Graphene Oxide (GO) Using the Tour Method with Different Parameters. *Advances in Materials Science and Engineering*. 2019;2019. doi:10.1155/2019/5058163

39. Raidongia K, Tan ATL, Huang J. Graphene Oxide: Some New Insights into an Old Material. *Carbon Nanotubes and Graphene: Edition 2*. Published online July 9, 2014:341-374. doi:10.1016/B978-0-08-098232-8.00014-0

40. Ray SC. Application and Uses of Graphene Oxide and Reduced Graphene Oxide. *Applications of Graphene and Graphene-Oxide Based Nanomaterials*. Published online 2015:39-55. doi:10.1016/B978-0-323-37521-4.00002-9

41. Randviir EP, Brownson DAC, Banks CE. A decade of graphene research: production, applications, and outlook. *Materials Today*. 2014;17(9):426-432. doi: 10.1016/J.MATTOD.2014.06.001

42. R. Roy, R. A Roy and D. M Roy, "Alternative Perspectives on “Quasi- Crystallinity”: Non-Uniformity and Nanocomposites,” Materials Letters, 4, 323-328 (1986) -

43. Huang J, Chen H, Fam D, et al. Growth of reduced graphene oxide. *Materials Research Society Symposium Proceedings*. 2014;1702. doi:10.1557/OPL.2014.854

44. Jahan M, Bao Q, Loh KP. Electrocatalytically active graphene-porphyrin MOF composite for oxygen reduction reaction. *J Am Chem Soc*. 2012;134(15):6707-6713. doi:10.1021/JA211433H
45. Lv X, Li S. Graphene Oxide-Crospolyvinylpyrrolidone Hybrid Microspheres for the Efficient Adsorption of 2,4,6-Trichlorophenol. *ACS Omega*. 2020;5(30):18862-18871. doi:10.1021/ACSOMEGA.0C02028
46. Jiang D, Chen Y, Li N, et al. Synthesis of luminescent graphene quantum dots with high quantum yield and their toxicity study. *PLoS ONE*. 2015;10(12). doi: 10.1371/JOURNAL.PONE.0144906
47. Bagri A, Mattevi C, Acik M, Chabal YJ, Chhowalla M, Shenoy VB. Structural evolution during the reduction of chemically derived graphene oxide. Published online 2010. doi:10.1038/NCHEM.686
48. Ren W, Fang Y, Wang E. A binary functional substrate for enrichment and ultrasensitive SERS spectroscopic detection of folic acid using graphene oxide/Ag nanoparticle hybrids. *ACS Nano*. 2011;5(8):6425-6433. doi:10.1021/NN201606R
49. Zhong T, Li J, Zhang K. A molecular dynamics study of Young's modulus of multilayer graphene. *Journal of Applied Physics*. 2019;125(17). doi:10.1063/1.5091753
50. Zheng Q, Geng Y, Wang S, Li Z, Kim JK. Effects of functional groups on the mechanical and wrinkling properties of graphene sheets. *Carbon N Y*. 2010; 48:4315-4322. doi: 10.1016/j.carbon.2010.07.044
51. Zhu X, Shan Y, Xiong S, Shen J, Wu X. Brianyoungite/Graphene Oxide Coordination Composites for High-Performance Cu2+ Adsorption and Tunable Deep-Red Photoluminescence. *ACS Applied Materials and Interfaces*. 2016;8(24):15848-15854. doi:10.1021/ACSAMI.6B05464
52. Zheng Q, Geng Y, Wang S, Li Z, Kim JK. Effects of functional groups on the mechanical and wrinkling properties of graphene sheets. *Carbon N Y*. 2010; 48:4315-4322. doi: 10.1016/j.carbon.2010.07.044
53. Suk JW, Piner RD, An J, Ruoff RS. Mechanical properties of monolayer graphene oxide. *ACS Nano*. 2010;4(11):6557-6564. doi:10.1021/NN101781V/ASSET/IMAGES/NN.
54. Al-Obaidi NS, Al-Garawi ZS, Al-Mahdawi AS. Polyaniline doping with nanoparticles: A review on the potential of electrical properties. *Journal of Physics: Conference Series*. 2021;1853(1):012055. doi:10.1088/1742-6596/1853/1/012055
55. Yang Y, Peng Y, Saleem MF, Chen Z, Sun W. Hexagonal Boron Nitride on III–V Compounds: A Review of the Synthesis and Applications. *Materials 2022, Vol 15, Page 4396*. 2022;15(13):4396. doi:10.3390/MA15134396
56. Fan ZJ, Kai W, Yan J, et al. Facile synthesis of graphene nanosheets via Fe reduction of exfoliated graphite oxide. *ACS Nano*. 2011;5(1):191-198. doi:10.1021/NN102339T
57. Yang J, Min M, Yoon Y, Kim WJ, Kim S, Lee H. Impermeable flexible liquid barrier film for

encapsulation of DSSC metal electrodes. *Scientific Reports 2016 6:1*. 2016;6(1):1-8. doi:10.1038/srep27422

58. Khalil I, Julkapli NM, Yehye WA, Basirun WJ, Bhargava SK. Graphene-Gold Nanoparticles Hybrid-Synthesis, Functionalization, and Application in a Electrochemical and Surface-Enhanced Raman Scattering Biosensor. *Materials (Basel)*. 2016;9(6). doi:10.3390/MA9060406

59. Herbut I. Electrons in graphene: an interacting fluid par excellence. *Physics (College Park Md)*. 2009;2. doi:10.1103/PHYSICS.2.57

60. Bolotin KI, Sikes KJ, Hone J, Stormer HL, Kim P. Temperature-dependent transport in suspended graphene. *Physical Review Letters*. 2008;101(9):096802. doi:10.1103/PHYSREVLETT.101.096802/FIGURES/4/MEDIUM

61. Tang L, Du D, Yang F, et al. Preparation of Graphene-Modified Acupuncture Needle and Its Application in Detecting Neurotransmitters. *Scientific Reports 2015 5:1*. 2015;5(1):1-9. doi:10.1038/srep11627

62. Herna¬ndez-Santos D, Begon*f*a Gonza¬lez-Garcìa M, Garcìa AC. Metal-Nanoparticles Based Electroanalysis. Published online 1996. doi:10.1002/1521-4109

63. Panigrahi S, Kundu S, Ghosh SK, Nath S, Pal T. General method of synthesis for metal nanoparticles. *Journal of Nanoparticle Research*. 2004;6(4):411-414. doi:10.1007/S11051-004-6575-2

64. Gade A, Ingle A, Whiteley C, Rai M. Mycogenic metal nanoparticles: Progress and applications. *Biotechnology Letters*. 2010;32(5):593-600. doi:10.1007/S10529-009-0197-9

65. Boles MA, Engel M, Talapin D v. Self-assembly of colloidal nanocrystals: From intricate structures to functional materials. *Chemical Reviews*. 2016;116(18):11220-11289. doi: 10.1021/ACS.CHEMREV.6B00196

66. Buonsanti R, Milliron DJ. Chemistry of doped colloidal nanocrystals. *Chemistry of Materials*. 2013;25(8):1305-1317. doi:10.1021/CM304104M

67. Kovalenko M v., Scheele M, Talapinl D v. Colloidal nanocrystals with molecular metal chalcogenide surface ligands. *Science (1979)*. 2009;324(5933):1417-1420. doi:10.1126/SCIENCE.1170524

68. Talapin D v., Lee JS, Kovalenko M v., Shevchenko E v. Prospects of colloidal nanocrystals for electronic and optoelectronic applications. *Chemical Reviews*. 2010;110(1):389-458. doi:10.1021/CR900137K

69. Ryzhii V, Ryzhii M, Otsuji T. Negative dynamic conductivity of graphene with optical pumping. *Journal of Applied Physics*. 2007;101(8):083114. doi:10.1063/1.2717566

70. Kelly KL, Coronado E, Zhao LL, Schatz GC. The optical properties of metal nanoparticles: The influence of size, shape, and dielectric environment. *Journal of Physical Chemistry B*. 2003;107(3):668-

677. doi: 10.1021/JP026731Y/ASSET/IMAGES/LARGE/JP026731YF00014.JPEG

71. Figure 1 | Nanobiosensors Based on Localized Surface Plasmon Resonance for Biomarker Detection

72. Li R, Fang D, Xu L, et al. Simulation of local surface plasmon resonance of single gold nano-disk. *2015 International Conference on Optoelectronics and Microelectronics, ICOM 2015*. Published online February 3, 2016:305-308. doi:10.1109/ICOOM.2015.7398828

73. Solomon SD, Bahadory M, Jeyarajasingam A v., Rutkowsky SA, Boritz C, Mulfinger L. Synthesis, and study of silver nanoparticles. *Journal of Chemical Education*. 2007;84(2):322-325. doi:10.1021/ED084P322

74. Cao T, Trefalt G, Borkovec M. Aggregation of Colloidal Particles in the Presence of Hydrophobic Anions: Importance of Attractive Non-DLVO Forces. *Langmuir*. 2018;34(47):14368-14377. doi: 10.1021/ACS.LANGMUIR.8B03191/ASSET/IMAGES/LARGE/LA-2018-03191A_0009.JPEG

75. Elimelech M, Gregory J, Jia X, Williams RA. Application of simulation techniques to colloidal dispersion systems. *Particle Deposition & Aggregation*. Published online January 1, 1995:402-425. doi:10.1016/B978-075067024-1/50015-7

76. Tan C, Huang X, Zhang H. Synthesis, and applications of graphene-based noble metal nanostructures. *Materials Today*. 2013;16(1-2):29-36. doi: 10.1016/J.MATTOD.2013.01.021

77. Zhu C, Dong S. Synthesis of graphene-supported noble metal hybrid nanostructures and their applications as advanced electrocatalysts for fuel cells. *Nanoscale*. 2013;5(22):10765-10775. doi:10.1039/C3NR03280A

78. Zhang M, Liu K, Xiang L, Lin Y, Su L, Mao L. Carbon nanotube-modified carbon fiber microelectrodes for in vivo voltammetric measurement of ascorbic acid in rat brain. *Anal Chem*. 2007;79(17):6559-6565. doi:10.1021/ac0705871

79. Zhang Z, Chen H, Xing C, et al. Sodium citrate: A universal reducing agent for reduction / decoration of graphene oxide with au nanoparticles. *Nano Research 2011 4:6*. 2011;4(6):599-611. doi:10.1007/S12274-011-0116-Y

80. Huang CK, Wu T, Huang CW, Lai CY, Wu MY, Lin YW. Enhanced photocatalytic performance of BiVO4 in aqueous AgNO3 solution under visible light irradiation. *Applied Surface Science*. 2017; 399:10-19. doi: 10.1016/J.APSUSC.2016.12.038

81. Huang X, El-Sayed MA. Gold nanoparticles: Optical properties and implementations in cancer diagnosis and photothermal therapy. *Journal of Advanced Research*. 2010;1(1):13-28. doi: 10.1016/J.JARE.2010.02.002

82. Zhang JJ, Gu MM, Zheng TT, Zhu JJ. Synthesis of gelatin-stabilized gold nanoparticles and

assembly of carboxylic single-walled carbon nanotubes/Au composites for cytosensing and drug uptake. *Analytical Chemistry*. 2009;81(16):6641-6648. doi:10.1021/AC900628Y

83. Han Z, Qi L, Shen G, Liu W, Chen Y. Determination of chromium (VI) by surface plasmon field-enhanced resonance light scattering. *Analytical Chemistry*. 2007;79(15):5862-5868. doi:10.1021/AC062453D

84. Goia D v., Matijević E. Preparation of monodispersed metal particles. *New Journal of Chemistry*. 1998;22(11):1203-1215. doi:10.1039/A709236I

85. Bashir O, Hussain S, Khan Z, Ahmed AL-Thabaiti S. Encapsulation of silver nanocomposites and effects of stabilizers. *Carbohydrate Polymers*. 2014; 107:167-173. doi: 10.1016/j.carbpol.2014.02.055

86. Bunaciu AA, Udriştioiu E gabriela, Aboul-Enein HY. X-Ray Diffraction: Instrumentation and Applications. *Critical Reviews in Analytical Chemistry*. 2015;45(4):289-299. doi:10.1080/10408347.2014.949616

87. L.Stobinski, B.Lesiak. A.Malolepszy, M.Mazurkiewicz, B.Mierzwa, J.Zemek, P.Jiricek, I.Bieloshapka: Graphene oxide and reduced graphene oxide studied by the XRD, TEM and electron spectroscopy methods Volume 195, August 2014, Pages 145-154 88. Elton LRB, Jackson DF. X-Ray Diffraction and the Bragg Law. *Citation: American Journal of Physics*. 1966; 34:1036. doi:10.1119/1.1972439

89. Lyon L, Keating C, Fox A, Baker B, … LHA, 1998 undefined. Raman spectroscopy. *academia.edu*.

90. Smith E, Dent G. *Modern Raman Spectroscopy: A Practical Approach*.; 2019.

91. Mulvaney SP, Keating CD. Raman spectroscopy. *Analytical Chemistry*. 2000;72(12). doi:10.1021/A10000155

92. York DLN, Raman spectroscopy (1977)

93. Mulvaney S, Chemistry CKA, 2000 undefined. Raman spectroscopy. *ACS Publications*.

94. Hanlon E, Manoharan R, … TKP in M, 2000 undefined. Prospects for in vivo Raman spectroscopy. *iopscience.iop.org*

95. ROSENBERG M, KOPELMAN IJ, TALMON Y. A Scanning Electron Microscopy Study of Microencapsulation. *Journal of Food Science*. 1985;50(1):139-144. doi:10.1111/J.1365-2621.1985.TB13295.X

96. Frankel RS, Aitken DW. Energy-Dispersive X-Ray Emission Spectroscopy. *Applied Spectroscopy*. 1970;24(6):557-566. doi:10.1366/000370270774372308

97. Williams R, … RHJ of the A, 2011 undefined. Quantification of the extent of reaction of metakaolin-based geopolymers using X-ray diffraction, scanning electron microscopy, and energy-dispersive spectroscopy. *Wiley Online Library*. 2011;94(8):2663-2670. doi:10.1111/j.1551-2916.2011.

04410.x

98. Pascarelli S, Mathon O, Munõz M, Mairs T, Susini J. Energy-dispersive absorption spectroscopy for hard-X-ray micro-XAS applications. *Journal of Synchrotron Radiation*. 2006;13(5):351-358. doi:10.1107/S0909049506026938

99. Ngo PD. Energy Dispersive Spectroscopy. *Failure Analysis of Integrated Circuits*. Published online 1999:205-215. doi:10.1007/978-1-4615-4919-2_12

100. Picollo M, Aceto M, Vitorino T. UV-Vis spectroscopy. *Physical Sciences Reviews*. 2019;4(4). doi:10.1515/PSR-2018-0008/HTML

101. protocols PMF, 1999 undefined. UV-visible spectroscopy as a tool to study flavoproteins. *Springer*.

102. Lai Q, Zhu S, Luo X, Zou M, Huang S. Ultraviolet-visible spectroscopy of graphene oxides. *AIP Advances*. 2012;2(3). doi:10.1063/1.4747817

103. Macheroux P. UV-visible spectroscopy as a tool to study flavoproteins. *Methods Mol Biol*. 1999; 131:1-7. doi:10.1385/1-59259-266-X:1

104. Ahmad A, Setapar S, … AYMT, 2021 undefined. Synthesis and characterization of GO-Ag nanocomposite for removal of malachite dye from aqueous solution. *Elsevier*. 105. Kumari S, Sharma P, Yadav S, et al. A Novel Synthesis of the Graphene Oxide-Silver (GO-Ag) Nanocomposite for Unique Physiochemical Applications. *ACS Omega*. 2020;5(10):5041-5047. doi: 10.1021/ACSOMEGA.9B03976/ASSET/IMAGES/LARGE/AO9B03976_0010.JPEG

106. Tan Thi P, Thang L van, van Khai T, et al. Synthesis of Ag/GO nanocomposite with promising photocatalytic ability for reduction reaction of p-nitrophenol. *Materials Research Express*. 2021;8(10):105009. doi:10.1088/2053-1591/AC2EAD